Title:

Effect of molecular exchange on water droplet size analysis as determined by diffusion NMR: the W/O/W double emulsion case

Abbreviations in the Title

NMR, Nuclear Magnetic Resonance; W/O/W, water-in-oil-in-water

Keywords:

molecular exchange; water exchange; tetramethylammonium chloride; water droplet size analysis; W/O/W emulsion (water-in-oil-in-water); diffusion NMR (Nuclear Magnetic Resonance); pfg-NMR diffusometry (pulsed field gradient); low-resolution NMR; high-resolution NMR

Authors names and affiliations:

Lien Vermeir[a*], Paolo Sabatino[a,b], Mathieu Balcaen[a], Arnout Declerck[a], Koen Dewettinck[c], José C. Martins[b], Gisela Guthausen[d] and Paul Van der Meeren[a]

("Van der Meeren" is the family name of author Paul Van der Meeren, the family names of the other authors are their last names as appear above)

[a] Particle and Interfacial Technology Group, Department of Applied Analytical and Physical Chemistry, Faculty of Bioscience Engineering, Ghent University, Coupure Links 653, B-9000 Ghent, Belgium

[b] NMR and Structure Analysis Unit, Department of Organic Chemistry, Faculty of Sciences, Ghent University, Krijgslaan 281 S4, B-9000 Ghent, Belgium

[c] Laboratory of Food Technology and Engineering, Department of Food Safety and Food Quality, Faculty of Bioscience Engineering, Ghent University, Coupure Links 653, B-9000 Ghent, Belgium

[d] Pro^{2}NMR, MVM and IBG-4, Karlsruher Institut für Technologie, Adenauerring 20b, DE-76131 Karlsruhe, Germany

Lien.Vermeir@UGent.be, P.Sabatino@yahoo.it, Mathieu.Balcaen@UGent.be, Arnout.Declerck@UGent.be, Koen.Dewettinck@UGent.be, Jose.Martins@UGent.be, Gisela.Guthausen@kit.edu, Paul.VanderMeeren@UGent.be

[*]**Corresponding author**. Particle and Interfacial Technology Group, Faculty of Bioscience Engineering, Ghent University, Coupure Links 653, B-9000 Ghent, Belgium. Tel.: +32 9 264 99 06. Email address: Lien.Vermeir@UGent.be

Highlights

- A multi-nuclear diffusion analysis of W/O/W emulsions was performed using diffusion NMR.
- The water diffusion signal was recorded by low and high-resolution NMR.
- The water-soluble marker diffusion signal was recorded by high-resolution NMR.
- Signal comparison enables the evaluation of molecular exchange.
- Signal analysis enables to determine the water droplet size of W/O/W emulsions.
- The latter's accuracy using water diffusion NMR depends on water exchange effects.

Graphical abstract

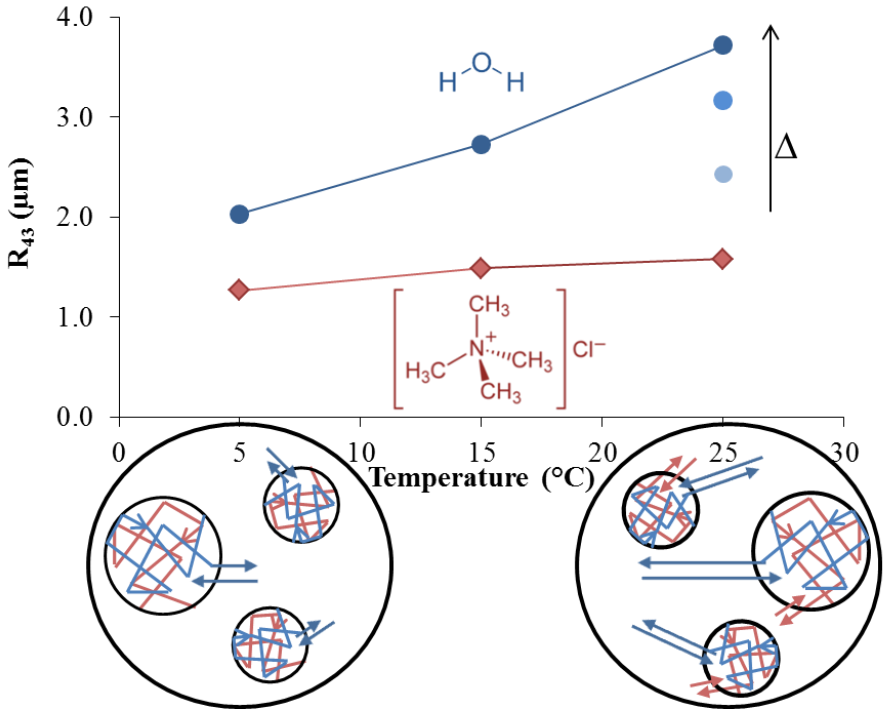

Title:

Effect of molecular exchange on water droplet size analysis as determined by diffusion NMR: the W/O/W double emulsion case

Abbreviations in the Title

NMR, Nuclear Magnetic Resonance; W/O/W, water-in-oil-in-water

Authors names and affiliations:

Lien Vermeir[a*], Paolo Sabatino[a,b], Mathieu Balcaen[a], Arnout Declerck[a], Koen Dewettinck[c], José C. Martins[b], Gisela Guthausen[d] and Paul Van der Meeren[a]

("Van der Meeren" is the family name of author Paul Van der Meeren, the family names of the other authors are their last names as appear above)

[a] Particle and Interfacial Technology Group, Department of Applied Analytical and Physical Chemistry, Faculty of Bioscience Engineering, Ghent University, Coupure Links 653, B-9000 Ghent, Belgium

[b] NMR and Structure Analysis Unit, Department of Organic Chemistry, Faculty of Sciences, Ghent University, Krijgslaan 281 S4, B-9000 Ghent, Belgium

[c] Laboratory of Food Technology and Engineering, Department of Food Safety and Food Quality, Faculty of Bioscience Engineering, Ghent University, Coupure Links 653, B-9000 Ghent, Belgium

[d] Pro^{2}NMR, MVM and IBG-4, Karlsruher Institut für Technologie, Adenauerring 20b, DE-76131 Karlsruhe, Germany

Lien.Vermeir@UGent.be, P.Sabatino@yahoo.it, Mathieu.Balcaen@UGent.be, Arnout.Declerck@UGent.be, Koen.Dewettinck@UGent.be, Jose.Martins@UGent.be, Gisela.Guthausen@kit.edu, Paul.VanderMeeren@UGent.be

[*]**Corresponding author**. Particle and Interfacial Technology Group, Faculty of Bioscience Engineering, Ghent University, Coupure Links 653, B-9000 Ghent, Belgium. Tel.: +32 9 264 99 06. Email address: Lien.Vermeir@UGent.be

Abstract

Hypothesis

The accuracy of the inner water droplet size determination of W/O/W emulsions upon water diffusion measurement by diffusion NMR was evaluated. The resulting droplet size data were compared to the results acquired from the diffusion measurement of a highly water soluble marker compound with low permeability in the oil layer of a W/O/W emulsion, which provide a closer representation of the actual droplet size. Differences in droplet size data obtained from water and the marker were ascribed to extra-droplet water diffusion.

Experiments

The diffusion data of the tetramethylammonium cation marker were measured using high-resolution pulsed field gradient NMR, whereas the water diffusion was measured using both low-resolution and high-resolution NMR. Different data analysis procedures were evaluated to correct for the effect of extra-droplet water diffusion on the accuracy of water droplet size analysis.

Findings

Using the water diffusion data, the use of a low measurement temperature and diffusion delay Δ could reduce the droplet size overestimation resulting from extra-droplet water diffusion, but this undesirable effect was inevitable. Detailed analysis of the diffusion data revealed that the extra-droplet diffusion effect was due to an exchange between the inner water phase and the oil phase, rather than by exchange between the internal and external aqueous phase. A promising data analysis procedure for retrieving reliable size data consisted of the application of Einstein's diffusion law to the experimentally determined diffusion distances. This simple procedure allowed determining the inner water droplet size of W/O/W emulsions upon measurement of water diffusion by low-resolution NMR at or even above room temperature.

Keywords: molecular exchange; water exchange; tetramethylammonium chloride; water droplet size analysis; W/O/W emulsion (water-in-oil-in-water); diffusion NMR (Nuclear Magnetic Resonance); pfg-NMR diffusometry (pulsed field gradient); low-resolution NMR; high-resolution NMR

Abbreviation in the text[1]

[1] NMR, Nuclear Magnetic Resonance; pfg, pulsed field gradient; W/O/W, water-in-oil-in-water; TMACl, tetramethylammonium chloride

1. Introduction

Water-in-oil-in-water (W/O/W) emulsions have the potential to create light foods as part of the oily dispersed phase is replaced by water [1]. In order to optimize the double emulsion formulation and to control its stability and functionality, the inner water droplet size distribution and internal water fraction can be determined. A wide range of emulsions in food process control and development have been characterized by low-resolution benchtop NMR [2]. The droplet size distribution of O/W, W/O, W/O/W and O/W/O emulsions can be determined using ^{1}H pulsed field gradient (pfg) NMR diffusometry [3-8]. Hereby, the droplet size distribution is estimated upon measurement of the restricted (intra-droplet) diffusion coefficient of molecules of the dispersed phase, followed by data analysis such as the procedure described by Murday and Cotts [9]. The latter procedure assumes that the droplet boundaries are impermeable. In addition, low-resolution NMR has also been applied to obtain information about the inner water volume fraction of W/O/W emulsions [6,10,11].

We have recently shown that molecular transport of water molecules through the oil layer of water-in-oil (W/O) emulsions can be detected using diffusion NMR [8]. This type of extra-droplet water diffusion was shown to become more important when raising the measurement temperature and NMR diffusion delay time Δ [6,8,12-14]. Extra-droplet water diffusion brought about an apparent increase in mean droplet size of W/O emulsions when using the Murday and Cotts data procedure [9], as well as when using the available data procedure that takes exchange into account [15]. These artefacts were unavoidable even when performing the diffusion analysis at low Δ and temperature. A data splicing procedure and the use of Einstein's diffusion law were proposed for determination of the droplet size, minimally affected by water exchange [8].

As W/O/W emulsions are more complex systems, it is interesting to evaluate whether the above mentioned instructs (i.e. low Δ and temperature) for minimizing the effect of extra-droplet water diffusion on the accuracy of water droplet size analysis also apply for W/O/W emulsions. For the same purpose, different data analysis procedures were evaluated. As a solid crystalline fat might suppress diffusion processes of water through the fat phase layer [16], the double emulsions were prepared either using a liquid oil or a solid fat.

To that end, both high-resolution NMR and low-resolution NMR, a more practical approach for measuring water diffusion, were applied. The former method enables the measurement of the spectrally-resolved diffusion signal of aqueous dissolved molecular species and water molecules in the water phases of W/O/W emulsions. Synchronous analysis of both signals allows the verification of the occurrence of molecular exchange. The water soluble tetramethylammonium chloride was selected, on account of an intense signal in a specific NMR region without overlap with water or oil, in addition to its low permeability through the oil phase due to its ionic nature [8,17-19].

To the best of our knowledge, this is the first simultaneous multi-nuclear temperature dependent diffusion analysis of water and a dissolved marker enclosed in W/O/W emulsion droplets as measured at different diffusion delays Δ using low-resolution and high-resolution pfg-NMR.

2. Materials and methods

2.1. Materials

The lipophilic emulsifier polyglycerol polyricinoleate (PGPR 4150; min. 75% n-glycerols with n = 2, 3 and 4; max. 10% m-glycerols with m $\geq$ 7) was kindly provided by Palsgaard A/S (Denmark). The hydrophilic emulsifier sodium caseinate (5.5% moisture; 96% protein on dry matter) was received as a gift sample from Armor Protéines (Saint Brice en Cogles, France), whereas Polysorbate 80 (Tween 80) was obtained from Sigma-Aldrich (Steinheim, Germany). High oleic sunflower oil (Hoso, Iodine Value = 87; 82% C18:1; SFC = 0% at 5 °C) was acquired from Contined B.V. (Bennekom, The Netherlands). Soft palm mid fraction (soft PMF; Iodine Value = 42-50; SFC = 79% at 5 °C) was purchased from Unigra Sp. (Conselice, Italy).

Tetramethylammonium chloride (TMACl, 109.6 g/mol) was obtained from Sigma-Aldrich (Steinheim, Germany). Deuterated water with a purity of 99.8 atom %D was purchased from Armar Chemicals (Switzerland). Food grade xanthan gum (FF) was a generous gift sample from Jungbunzlauer (Vienna, Austria). The 0.1 M phosphate buffer solution (pH 6.7) contained 0.02% (w/v) of the anti-microbial agent NaN_3 (Acros Organics, Geel, Belgium), KH_2PO_4 (Merck KGaA, Darmstadt, Germany) and K_2HPO_4 (Alfa Aesar, Karlsruhe, Germany). Unless stated differently, the above mentioned chemicals were of analytical grade.

2.2. Sample preparation

The inner (W_1) and outer (W_2) water phase of the $W_1/O/W_2$ emulsions that were investigated by both high and low-resolution NMR contained 800 mM TMACl in a mixture of D_2O/H_2O (50:50, wt%). In addition, the W_2 phase contained 0.2 wt% xanthan gum and 1.4 wt% Tween 80. The oil phase consisted of 2.5 wt% PGPR in Hoso. The W_1/O emulsions (40 g of 50:50, w/w) were mixed at 60 °C with an Ultra-Turrax (type S25KV - 25G, IKA®-Werke, Germany) at 6500 rpm for 4 min. The $W_1/O/W_2$ (30 g of 20:20:60, w/w) was prepared at room temperature upon mixing the W_1/O emulsion with W_2 phase with an Ultra-Turrax (type S25-10G, IKA®-Werke, Germany) at 9500 rpm for 1 min.

Regarding the composition of emulsions investigated only by low-resolution NMR, reference is made to the procedure described by Su et al. [20], which differs in the applied phase ratio and surfactant concentration. An Ultra-Turrax (type S 50 N - G 45 F, IKA®-Werke, Germany) and a Microfluidizer (type

M110S, Microfluidics) at 840 bar (driving air pressure of 6 bar) for 1.5 min were used to premix and homogenize the W_1/O emulsion (160 g, 50:50, w/w) at 60 °C, respectively. The primary water phase (W_1) contained 1.25% (w/v) sodium caseinate and 0.1 M phosphate buffer solution, whereas the fat phase consisted of 2.5% (w/v) PGPR in soft PMF or Hoso. The $W_1/O/W_2$ (100 g) emulsion was prepared at room temperature upon mixing the external water phase (W_2) with freshly prepared W_1/O emulsion in a 60:40 (w/w) ratio with an Ultra-Turrax S25-10G (IKA®-Werke, Germany) at 13500 rpm for 1 minute. Hereby, the W_2 phase only differs from the W_1 phase in the concentration of sodium caseinate (1%, w/v). Afterwards, all double emulsions were further mixed with a continuous Ultra-Turrax DK25 (IKA®-Werke, Germany) at 13500 rpm for 1 minute.

All samples were cooled in an ice/water bath for 40 minutes and subsequently stored in the refrigerator.

2.3. High-resolution NMR

High-resolution pfg-NMR diffusion analysis was performed with a Bruker Avance III spectrometer operating at a ^1H frequency of 500.13 MHz and equipped with a 5 mm DIFF30 gradient probe with a maximum gradient strength of 18 T/m. Measurements were performed at 5, 15 or 25 °C and the temperature was controlled to within ± 0.01 °C with a Eurotherm 3000 VT digital controller. The samples (560 to 650 µL) were filled in 5 mm diameter glass NMR-tubes (Armar Chemicals, Switzerland). Pulsed field gradient (pfg) NMR experiments were performed using the conventional single stimulated echo pulse sequence. The applied δ and Δ for the Tween 80-stabilized W/O/W emulsion was 4.5 ms and 250-450-600 ms, respectively. The free self-diffusion coefficient of water and TMACl in the water phase (W_1) was measured (D_s) upon varying G between 0.03 and 1.3 T/m while keeping δ and Δ constant at 1 ms and 50 ms, respectively ($D_{s,\,water}$ = 1.14 x 10^{-9}, 1.53 x 10^{-9} and 2.00 x 10^{-9} m^2/s at 5, 15 and 25 °C and $D_{s,\,TMACl}$ = 5.10 x 10^{-10}, 7.03 x 10^{-10} and 9.01 x 10^{-10} m^2/s, respectively).

2.4. Low-resolution NMR

NMR measurements were performed on a benchtop Maran Ultra spectrometer (Oxford Instruments, UK) operating at a frequency of 23.4 MHz. The samples were adequately filled [11] in 18 mm diameter glass NMR-tubes (Oxford Instruments, UK). Pulsed field gradient (pfg) NMR experiments were performed using the stimulated echo pulse (STE) sequence, which was preceded by an inversion recovery experiment for suppression of the NMR-signal from the fat phase in the emulsion, characterized by a time period τ_{null} [2]. Measurements were performed varying the gradient strength (G) [21] between 0 and 3.17 T/m. The applied δ and Δ for the experiment on sodium caseinate stabilized W/O/W emulsions was 2.5 ms and 60-80-100-140-220 ms, respectively. In order to enable comparison with the high-resolution NMR experiment, higher values of δ and Δ were applied for the measurement of the Tween 80-stabilized

W/O/W emulsions, i.e. 4.5 ms and 240-440-600 ms, respectively. For the other applied NMR parameters we refer to [11]. The free self-diffusion coefficient of the water phases was measured (D_s) using the DSD script (Oxford Instruments, UK) and varying δ between 0.05 and 2.75 ms while keeping G and Δ constant at 0.14 T/m and 200 ms, respectively. The D_s of the W_1 phase containing 1.25% sodium caseinate in 0.1 M phosphate buffer solution amounted to 1.20 x 10^{-9}, 1.75 x 10^{-9}, 2.29 x 10^{-9} and 2.82 x 10^{-9} m^2/s at 5, 15, 25 and 35 °C, respectively. The D_s values of the 800 mM TMACl containing W_1 phase amounted to 8.82 x 10^{-10}, 1.23 x 10^{-9} and 1.58 x 10^{-9} m^2/s at 5, 15 and 25 °C. These values roughly comply with the weighted average of the $D_{s,\,water}$ and $D_{s,\,TMACl}$ as obtained from high-resolution NMR. Using a H-molar concentration for H_2O of 55.6 mol H per liter (i.e. ½ x 55.6 mol/L x 2 mol H/mol), a H-molar concentration for TMACl of 9.6 mol H per liter (i.e. 0.8 mol/L x 12 mol H/mol) and a fraction for water of 55.6/(55.6+9.6), the weighted average amounts to 1.05 x 10^{-9}, 1.41 x 10^{-9} and 1.84 x 10^{-9} m^2/s at 5, 15 and 25 °C, respectively.

2.5. Statistical analysis

Unless stated differently, the uncertainty of the estimated values and error bars in the graphs represent the standard error of the estimates. The latter values were obtained directly from the Matlab fitting procedure, by the Monte Carlo method [22] or by linear regression in Excel (Microsoft Office 2010), from which a 95% confidence interval could be constructed. Regarding the comparison of model fitting with a different number of parameters of the diffusion data, the applied measure of goodness-of-fit was the root mean squared error (RMSE), whereas the fit to relative trend was measured by the adjusted R^2-value.

3. Background theory

Differences in diffusion behavior in W/O/W emulsions allow discriminating between internal and external water. Water molecules in the external water phase experience quasi free diffusion ('FW') (with a minor obstruction effect due the oil globules present) characterized by D_e, whereas the diffusion in the internal water droplets is restricted. The latter can be described by the Murday and Cotts equation E_{MC} [9,23,24], assuming that the diffusion of the inner water droplets, as well as the water exchange through the oil or fat phase is negligible during the analysis (Fig. 1a). A full expression of E_{MC} can be found in [24].

Provided that the two water compartments can be regarded as independent [11], a combination of fast and slow echo decay is recorded at low and high values of q^2, respectively, and the water signal should give rise to a quasi bi-component decay E_{MCFW} (Eq. (1)) as a function of q^2 and diffusion delay Δ.

$$E_{MCFW}(q^2,\Delta) = \frac{I}{I_0} = EV \cdot \frac{\int_0^\infty P_v(R) \cdot E_{MC}(R,q^2,\Delta)dR}{\int_0^\infty P_v(R)\,dR} + (1-EV)\cdot \exp\left(-q^2 \cdot \left(\Delta - \frac{\delta}{3}\right) \cdot D_e\right) \qquad (1)$$

The amplitudes of the echo decay yield the enclosed water volume fraction, which is the fraction of the total water that is present as internal water droplets. To account for polydisperse droplet sizes, the normalized attenuation of the NMR signal I/I_0 of the population of possible spherical droplet radii R with a certain probability P_v can be described by the first term in Eq. (1) [3,24,25]. Hereby, P_v is usually modelled by a lognormal volume-weighted particle size distribution (Eq. (2a)), I_0 is the echo intensity in the absence of a magnetic field and q is a function of the gyromagnetic ratio γ (2.675 x 10^8 s^{-1} T^{-1}), the gradient duration δ and the gradient strength G according to $q^2 = (\delta \cdot \gamma \cdot G)^2$. The geometric mean radius (R_{33}) and geometric standard deviation (σ_g) in Eq. (2a) were converted to the arithmetic mean radius (R_{43}) and arithmetic standard deviation (σ) of the lognormal volume-weighted particle size distribution using Eqs. (2b,c).

$$P_v(R) = \frac{1}{\sqrt{2\pi}\cdot R \cdot \ln\,\sigma_g} \cdot \exp\left(-\frac{\left(ln(R) - ln(R_{33})\right)^2}{2\cdot\left(\ln\,\sigma_g\right)^2}\right) \tag{2a}$$

$$R_{43} = R_{33} \cdot \exp\left(\frac{\left(\ln\,\sigma_g\right)^2}{2}\right) \tag{2b}$$

$$\sigma = \sqrt{R_{43}^2 \cdot \left(exp\left(\left(\ln\,\sigma_g\right)^2\right) - 1\right)} \tag{2c}$$

The values for EV, R_{43}, I_0 and the effective diffusion coefficient in the outer aqueous phase (D_e) were determined upon performing a least-squares fit of Eq. (1) to the echo intensity data as measured for a certain Δ using Matlab 7.5.0.342 (R2007b) software (The MathWorks). For reasons of unreliable estimations, the arithmetic standard deviation σ was estimated upon fitting the first term of Eq. (1) (with EV = 100%) to the echo decay of the associated primary W/O emulsion; the best fitted σ-values are mentioned in [8].

In case that exchange occurs between two compartments, the exchange model as described by Pfeuffer et al. [15] and Schoberth et al. [26] can accommodate the diffusion behavior of water in the inner compartment, with finite water permeability, surrounded by external water:

$$E_{Pf}(q^2,\Delta) = p_1' \cdot \exp\left(-q^2 \cdot \left(\Delta - \frac{\delta}{3}\right) \cdot D_1'\right) + p_2' \cdot \exp\left(-q^2 \cdot \left(\Delta - \frac{\delta}{3}\right) \cdot D_2'\right) \tag{3}$$

Prime symbols indicate the parameters influenced by exchange of molecules and are henceforth termed apparent parameters. As such, the amplitudes and slopes of the echo decay will yield apparent water volume fractions ($p_{1,2}'$) and apparent diffusion coefficients of the inner and outer compartments ($D_{1,2}'$), which are functions of their real values ($p_{1,2}$ and $D_{1,2}$) and the mean residence time ($\tau_{1,2}$) in the internal and external water pool [8]. Hereby, D_1 (and the inner compartmental size distribution) results from taking

the partial derivative of the first term of Eq. (1) with respect to q^2. Consequently, molecular exchange can be observed when D_1 and D_2 differ and the concentrations in both compartments and of exchanging molecules are large enough.

4. Results and discussion

4.1. Exchange model selection

In literature, the exchange model (Eq. (3)) has been applied to describe the diffusion signal of water exchanging between the two water phases of a W/O/W emulsion [10]. Assuming that the volume fraction of water in oil can be considered negligible [7], the values of $p_{1,2}$, $p'_{1,2}$, $D_{1,2}$, $D'_{1,2}$ and $\tau_{1,2}$ are associated with the inner and outer water pool. Simulation of the normalized NMR echo decay as a function of q^2 using Eq. (3) is shown in Fig. 2a. The simulated echo decay is characterized by two slopes, a larger slope at low q^2 and a smaller slope at large q^2 values. The slope of the fast decaying part increases for increasing Δ, whereas the slope of the slower part remains constant, but its amplitude decreases as attributed to extra-droplet diffusion of water through the oil layer inside the multiple droplets, as well as between the inner and outer water compartment. This statement is valid as long as there is exchange between the two water phases during the diffusion time Δ (dashed-dotted lines in Fig. 2a).

The simulated signal decays strongly change when water exchange between the two water phases is negligible during Δ, but primarily occurs between the inner water droplets and the oil phase (full lines in Fig. 2a). The extrapolated value for $q \rightarrow 0$ reflects the relative amplitudes of inner and outer water phases which should be independent of the values of the experimental NMR parameters. The NMR attenuation data of the double emulsions in our study exhibited the expected distinct echo decays. Fig. 2b shows that the slope of the slowly decreasing part of the echo decay of the sodium caseinate stabilized double emulsion as measured at 35 °C increased as the diffusion delay was increased and showed a common intercept. The former points to considerable extra-droplet exchange inside the multiple droplets, whereas the latter indicates that the exchange between the inner and outer water compartment was negligible within the time frame considered (i.e. two independent water compartments). Moreover, it suggests that the amplitudes of the echo decay related to the real enclosed water volume fraction remain constant over time, i.e. the molecular exchange is a phenomenon in a stable emulsion.

When neglecting the size distribution, the slope at high q^2 values indicate the droplet size. Hereby, the slope (and 95% confidence interval) of this slowly decreasing part amounted to -0.8 ± 0.1, -1.3 ± 0.1 and -1.8 ± 0.1 μm^2 at Δ of 60, 140 and 220 ms, whereas the slope of the fast decaying part amounted to -83 ± 13, -93 ± 48 and -93 ± 69 μm^2, respectively.

Upon extending the exchange model with a free water diffusion term, all three phases are considered, i.e. water molecules in the inner and outer water phases as well as in the oil phase. This extended model was able to fit the experimentally obtained echo decays in Fig. 2b:

$$E(q^2,\Delta) = \frac{I}{I_0} = EV \cdot E_{Pf}(q^2,\Delta) + (1 - EV) \cdot \exp\left(-q^2 \cdot \left(\Delta - \frac{\delta}{3}\right) \cdot D_3\right) \quad (4)$$

The first term of Eq. (4) contains the parameters influenced by exchange between water droplets (1st pool) and the oil layer (2nd pool) inside the oil droplets of the W/O/W emulsion, whereas the second term yields the effective diffusion coefficient D_3 of the external water phase (3rd pool), similar to D_e in Eq. (1). A schematic representation of Eq. (4) and its simulated diffusion echo signal decays are given in Fig. 1b and Fig. 2a, respectively.

The values of R_{43}, σ, τ_1, p_2, I_0, D_2, EV and D_3 were determined upon performing a least-squares fit of Eq. (4) to the echo intensity data as measured for a series of Δ using Matlab 7.5.0.342 (R2007b) software (The MathWorks). The water volume fraction in the inner water phase (p_1) and the mean residence time of water in the oil layer (τ_2) follow from $p_1 = 1 - p_2$ and $\tau_2 = \tau_1 \cdot \frac{1-p_1}{p_1}$, respectively. D_1 as a function of q^2 results from taking the partial derivative of the first term of Eq. (1) with respect to q^2 using the estimated R_{43} and σ.

In other studies [6,10], Eq. (3) was applied to fit the diffusion data of W/O/W emulsions to describe the exchange between internal and external water. The requirement of an extension of the exchange model (Eq. (4)) in which only exchange between the internal water and the oil phase is considered is explained by our different experimental settings and emulsion recipe as compared to others [6,10]. It is widely known that the double emulsion characteristics, and hence its diffusion signals, are strongly affected by the actual emulsion composition and preparation method. In our case, the 20:20:60 W/O/W emulsions with an external water phase either containing sodium caseinate without xanthan, sodium caseinate with 0.2% xanthan (data not shown) or Tween 80 with 0.2% xanthan showed the features as shown in Fig. 2b, which according to simulation (Fig. 2a) results from exchange between the internal water and oil phase, rather than from exchange between internal and external water phase.

4.2. Water versus tetramethylammonium chloride diffusion

In order to confirm the interpretation of the signal decays in section 4.1 independently, a tracer diffusion study was performed additionally. To study the water and marker compound diffusion in W/O/W emulsions, low and high-resolution pfg-NMR diffusometry were applied. Low-resolution NMR predominantly measures the diffusion of water molecules, whereas high-resolution NMR enables separate diffusion analysis of all ingredients separately due to chemical shift dispersion. I.e. water and water

soluble compounds as well as oil can be analyzed separately. This opens interesting perspectives since water soluble ionic marker molecules have a reduced permeability in hydrophobic media as oil in comparison to water molecules [19,27]. Ion transport through the oil film in W/O/W emulsions was shown to be driven by the osmotic pressure gradient across the oil film. Without osmotic pressure, its transport became hardly observable [28]. Upon addition of tetramethylammonium chloride to the inner and outer water phase of the W/O/W emulsion at the same concentration, the resulting marker diffusion signal associated with the inner water compartment is expected to reflect the maximum travelled distance that is Δ-independent and only affected by the droplet size, shape and compartmental water fractions, provided that the diffusion delay value is sufficiently long [18,19].

4.2.1. High-resolution NMR of Tween 80-stabilized W/O/W emulsions

The measured NMR echo decays of water and TMACl of the W/O/W emulsion at 5 °C are shown in Fig. 3. Upon fitting of Eq. (1) to the water and marker diffusion signals, markedly different estimated water droplet size values are obtained. The best fitted R_{43}-value (with 95% confidence) amounted to 2.03 ± 0.04 µm and 1.27 ± 0.08 µm, respectively. The estimated enclosed water volume fraction amounted to 32 ± 1% and 29 ± 4%, respectively.

The effect of diffusion delay (250-450-600 ms) on the NMR echo decay of the W/O/W emulsion at 25 °C is shown in Fig. 4. The curves in Fig. 4a show a continuous increase in slope for $q \rightarrow 0$. Considering a q^2 range of up to 20 x 10^{12} m^{-2}, the diffusion data of the marker in Fig. 4b were less affected by Δ.

The best fitted R_{43}-values of the inner water droplets of the double emulsion are given in Fig. 5, which were similar to the values as obtained upon fitting Eq. (1) to the echo decay while neglecting the first few points at very small q^2. This further sustains the argument of independent water compartments. A much larger apparent increase in R_{43}-value with increasing temperature and/or Δ was observed for water than for the marker (Fig. 5). Two different types of diffusion might result in an apparent increase in droplet size, i.e. extra-droplet water diffusion (either by molecular transport or surfactant facilitated diffusion) as well as diffusion of the water droplets themselves by thermal agitation [24]. In fact, droplet movement by thermal agitation is expected to influence both sets of estimated radii as obtained from the water and TMACl diffusion data in the same way. As the water diffusion data are clearly much more influenced by an increase in temperature in Fig. 5, it follows that the mechanism responsible for the observed apparent size increase is related to a finite permeability of the species through oil during Δ.

The temperature-induced increase originates from a more Gaussian diffusing signal following an increase in solubility and diffusivity of water through oil with measurement temperature [29,30]. In contrast, the permeability of ionic marker molecules is significantly lower as attributed to a reduced solubility in hydrophobic media [19,27].

In comparison to 25 °C and 15 °C, the overestimation of the droplet size using the water signal was decreased at 5 °C. The remaining difference of the radius based on the water and marker signal at 5 °C, however, designates that the use of a low temperature cannot avoid the effects of extra-droplet water diffusion on the estimated droplet size using the water signal.

The Δ-induced increase of the estimated droplet size can be ascribed to the magnifying effect of Δ on the diffusion signal when molecular exchange occurs [18,19,31]. Consequently, the overestimation of the water droplet size based on the water signal as measured at 25 °C was less pronounced when using lower Δ values. As the marker signal resulted in a much lower R_{43}-dependency of temperature and Δ, it is thought to approximate the real water droplet radius.

4.2.2. Low-resolution NMR of Tween 80-stabilized W/O/W emulsions

Low-resolution NMR was applied on the W/O/W emulsion as a function of temperature at Δ = 600 ms (Fig. 5). The water signal resulted in the same trend of the estimated R_{43}-value as a function of temperature as in the HR-NMR experiment. It is worth mentioning that the complete sample volume was detected using low-resolution NMR. Therefore, the amplitudes of the fitting of Eq. (1) to the LR-NMR echo decay were used to estimate the EV. The EV was hardly affected by the measurement temperature (5-15-25 °C) using a diffusion delay Δ of 600 ms, nor by diffusion delay Δ (240-440-600 ms) at a temperature of 25 °C; all EV-values were in the range of 26.6 to 28.5%, with no significant effect of Δ and temperature. This observation further sustains the lack of exchange between the internal and external aqueous phase in our double emulsions, as was already claimed in section 4.1.

4.3. Water exchange modeling

To evaluate water exchange in W/O/W emulsions, different models were applied to fit the low-resolution NMR water diffusion data as measured at different diffusion delays and temperatures. Hereby, the objective was to perform accurate droplet size analysis, which requires disentanglement of the effect of water exchange on the best fitted values.

As a first procedure, the results of the application of a non-exchange (Eq. (1)) and exchange model (Eq. (4)) were compared. The soft PMF based ($W/O_s/W$) and the Hoso-based ($W/O_h/W$) samples, of which the outer interface was stabilized by sodium caseinate, as kept at 5 °C, were heated to 15, 25 and 35 °C. At each holding temperature, the diffusion data were recorded for Δ values between 60 and 220 ms. The fitting of Eq. (1) and Eq. (4) is shown for the $W/O_s/W$ emulsion in Fig. 6, for which the R^2_{adj} and RMSE amounted to at least 0.991 and at most 0.104 (at 5, 15 and 35 °C), except for the $W/O_s/W$ emulsion at 25 °C using Eq. (1), for which it amounted to 0.910 and 0.339, respectively. Hereby, the latter deviating

values are mainly due to the fitting results of the $W/O_s/W$ emulsion using Δ of 60 ms and 100 ms, for which larger uncertainties of the best fitted radius R_{43} are shown in Fig. 7a.

The best fitted radius R_{43} of the inner droplets of the W/O/W emulsions clearly increased with increasing measurement temperature, which became more obvious using larger Δ-values (Fig. 7). This effect might proceed from an increased water permeability through the oil, connected with an increased water saturation solubility and water diffusion coefficient in vegetable oil with increasing temperatures [29,30]. This was further evidenced by measurement of the emulsions upon cooling to 5 °C after previous measurements at higher temperatures. The droplet size of the cooled emulsions was comparable to the original non-heated sample; the sample averaged droplet size of the cooled $W/O_s/W$ and $W/O_h/W$ emulsion amounted to 1.11 ± 0.08 µm and 1.93 ± 0.05 µm, respectively. Therefore, the observed increase in droplet size at higher temperatures must originate from increased water exchange rather than a real temperature-induced increase in droplet size.

The results also indicate that an increased solid fat content (SFC) of the fat phase could not guarantee a less pronounced apparent droplet size increase. Hereby, the $W/O_s/W$ emulsion at the lowest temperatures (5 and 15 °C) is characterized by a very large viscosity due to the fat crystal network. In fact, the SFC of soft PMF at 5 and 15 °C amounted to 65% and 56%, whereas it amounted to 0% for Hoso oil as determined by pulsed NMR [11]. Based on the study of Kiokias et al. [32], diffusion of oil molecules in an oil phase with a SFC larger than 50% is restricted due to the fat network microstructure. Upon extrapolation towards W/O/W emulsions, it can be assumed that water droplets (much larger in size than oil molecules) in W/O/W emulsions with a SFC > 50% will also be largely restricted in their diffusion, if not completely immobilized in the solid fat matrix. As such, the apparent droplet size increase of the $W/O_s/W$ emulsion at low temperatures can only be explained by extra-droplet water diffusion.

The application of Eq. (4) resulted in a slightly less pronounced temperature effect on the best fitted radius of the W/O/W emulsion (Fig. 7). However, the extended exchange model could only partly compensate for the effect of exchange on the droplet size, despite that it is designed to take exchange into account. The residence times of water in the inner water compartment of the W/O/W emulsions in Table 1 decreased with increasing temperature. Similar to the primary W/O emulsions in [8], the water residence times measured at low sample temperature, as well as their estimation error, are much larger than the diffusion time, which indicates a small effect of water exchange on the droplet size.

Pertaining to the geometric standard deviation σ_g of the $W/O_h/W$ emulsions, the best fitted values using Eq. (4) were relatively temperature independent (σ_g = 1.07 ± 0.05), unlike the $W/O_s/W$ emulsions, whose σ_g at 5 °C (σ_g = 1.49) and 15 °C (σ_g = 1.38) were larger than at 25 °C and 35 °C (for both σ_g = 1.00).

A second procedure was attempted to disentangle the estimated radius from the effect of exchange by means of a data splicing procedure. The procedure assumes that the diffusion data sets as measured at different temperatures and Δ originate from the same droplet size distribution. Upon jointly fitting the data to Eq. (4), a collective volume-weighted average droplet size is obtained, which amounted to 1.50 µm and 2.27 µm for W/O_s/W and W/O_h/W emulsion, respectively. As these values are significantly larger as compared to the experimental values obtained using Eq. (1) at low temperatures and low diffusion delay values, it follows that this procedure is not capable to completely eliminate extra-droplet water diffusion effects. Moreover, this data-splicing procedure has got the drawbacks to be complex, time-consuming and to hardly attach value to the data measured at higher temperature.

A third data analysis procedure to obtain a temperature independent radius assumes that the apparent increase in inner water droplet size is due to water diffusion through the oil phase. We have shown before that the distance travelled by diffusion in W/O emulsions could be corrected using Einstein's diffusion law (Eq. (5)) [33], which resulted in a diffusion delay independent droplet size ($R_{43,0}$), which is thought to approximate the real inner water droplet size [8].

$$R_{43}(T,\Delta) - R_{43,0}(T,\Delta = 0\ ms) = \sqrt{D(T)\cdot\Delta} \quad (5)$$

In Fig. 8, a least-squares fit of Eq. (5) to the R_{43}-values of the W/O_h/W emulsion (as obtained from Eq. (1) at constant temperature) is presented. Table 2 indicates that the extrapolated intercept ($R_{43,0}$) is temperature independent. Fig. 7a shows the best fitted $R_{43,0}$-value of the W/O_s/W emulsion at 5 °C, which was about 0.3 µm smaller than the R_{43} obtained from Eq. (1) at Δ of 60 to 100 ms. The larger estimated radius $R_{43,0}$ and error margin at 25 °C are mainly due to the fitting results of the W/O_s/W emulsion using Δ of 60 ms and 100 ms. Fig. 7b includes the results for the W/O_h/W emulsion, for which the estimated radius $R_{43,0}$ was similar to the R_{43} obtained from Eq. (1) at 5 °C.

The best fitted diffusion coefficient values (D) mostly increased with increasing temperature according to an Arrhenius-type relationship (Table 2). Excluding the W/O_s/W data at 25 °C, the resulting activation energy (with 95% confidence) was E_a = 68 ± 267 kJ/mol (R^2 = 0.914), which was about 1.4 times smaller than for the W/O_h/W emulsion (E_a = 95 ± 32 kJ/mol, R^2 = 0.988). As a similar difference in E_a was previously noted between the W/O_s (Ea = 79 ± 14 kJ/mol, R^2 = 0.997) and W/O_h emulsion (Ea = 121 ± 88 kJ/mol, R^2 = 0.947) [8], the obtained values of D and E_a indicate that diffusion of water through the oil layer might depend on the fat phase composition.

The Stokes Einstein equation ($D = \frac{k_B \cdot T}{6 \cdot \pi \cdot \eta \cdot r}$ with the diffusion coefficient D of the sphere with effective hydrodynamic radius r, the dynamic viscosity of the surrounding fluid η and Boltzmann's constant k_B [33])

can be used to further elucidate the dominating type of diffusion related to the apparent increase in droplet size. As the volume-weighted average radius of the water droplets of the $W/O_h/W$ emulsion as measured at 25 °C amounted to 2.06 µm (Table 2), their diffusion coefficient in sunflower oil of 0.05 Pa·s at 298 K [34] is 2.1 x 10^{-15} m^2/s. Fitting Eq. (5) to the experimental data resulted in a diffusion coefficient of 1.3 x 10^{-12} m^2/s (Table 2), which is three orders of magnitude larger than expected for water droplet diffusion in oil and hence, too large to describe the diffusion of micrometer-sized water droplets in oil. Using the Stokes-Einstein equation, the diffusion coefficient obtained by fitting Eq. (5) corresponded to a hydrodynamic radius r of 34 Å in sunflower oil. Regarding molecular water transport, the diameter of a water molecule is typically in the order of an Å. In case of surfactant facilitated diffusion of water (i.e. water transport by hydrated PGPR molecules or PGPR micelles) [35], the estimated radius strongly depends on the degree of polymerization of the considered PGPR. Using a hydrodynamic radius of a few nanometers for PGPR-facilitated water transport, the diffusion coefficient is in the order of 10^{-11} to 10^{-13} m^2/s. Hence, the hydrodynamic radii as estimated for extra-droplet water diffusion (i.e. molecular water transport or PGPR-facilitated water diffusion) indicate that the obtained diffusion coefficients from Eq. (5) must describe the diffusion of water through the oil layer.

5. Conclusions

A first objective was to evaluate the accuracy of water droplet size analysis of W/O/W emulsions using water diffusion NMR. Low-resolution and high-resolution diffusion NMR were applied to measure the diffusion data of water and the ionic aqueous dissolved marker tetramethylammonium chloride in the water phases of the W/O/W emulsion. Based on the fact that tetramethylammonium chloride has been shown to be an appropriate water soluble marker for NMR studies of emulsions on account of its low permeability through the oil phase in comparison to water [17-19], a previous NMR diffusion study of water and tetramethylammonium chloride in W/O emulsions revealed that the measurement temperature and Δ were crucial aspects towards obtaining more accurate water droplet size analysis using the water diffusion data [8]. It is interesting to find that these aspects were likewise important for W/O/W emulsions, albeit these systems are more complex as obtained upon emulsification of the W/O emulsion into an external water phase. The results depicted a much larger apparent increase in inner water droplet size of the W/O/W emulsion with increasing temperature and Δ in comparison to the use of the marker data.

It was postulated that the different observations between water and the marker were due to a more marked exchange of water through the oil layer inside the oil droplets in comparison to the marker during the diffusion analysis time. Consequently, the use of the latter's diffusion data is thought to approximate the real water droplet radius. Analysis at low temperature and Δ could reduce the droplet size overestimation

using the water diffusion data [6,8,12-14], but we showed that an overestimation was inevitable arising from extra-droplet water diffusion. Whereas a solid crystalline fat phase might slow down the water exchange kinetics in double emulsions [16], we demonstrated that an increased solid fat content of up to 65% was not sufficient to suppress water exchange through the fat layer.

A second objective was to investigate the capability of data analysis procedures to compensate for the effect of extra-droplet water diffusion. In previous studies [6,10], the exchange model was applied that considers exchange between internal and external water. Detailed diffusion analysis revealed that water exchange dominantly occurred between the internal water and the oil phase in our double emulsions during the time frame of the analysis. Therefore, an extension of the exchange model was proposed, but this model could only partly compensate for the effect of exchange in a three phase system. In addition, we showed that the very simple diffusion model, based on Einstein's diffusion law, enabled to regain a diffusion delay independent droplet size from droplet data obtained using a non-exchange model. Hereby, the use of Einstein's diffusion model provided a means to characterize the fat phase permeability of an emulsion, which may be used as an accessory during food product development and quality monitoring.

Acknowledgments

Research funded by a PhD grant (111 508) to L.V. of the Agency for Innovation by Science and Technology (IWT). The authors thank the Fund for Scientific Research – Flanders (FWO Vlaanderen) for their financial support for obtaining the low-resolution 23.4 MHz NMR equipment. We also acknowledge funding from Flanders' Food. Hercules foundation is acknowledged for its financial support in the acquisition of the high-resolution 500 MHz NMR equipment (grant number AUGE-09-006). G.G. would like to thank the Deutsche Forschungsgemeinschaft (DFG) for financial support within the instrumental facility Pro^{2}NMR.

References

[1] E. Dickinson, Food Biophysics 6 (2011) 1-11.

[2] J. P. M. van Duynhoven, G. J. W. Goudappel, G. van Dalen, P. C. van Bruggen, J. C. G. Blonk, A. P. A. M. Eijkelenboom, Magn. Reson. Chem. 40 (2002) S51-S59. DOI: 10.1002/mrc.1115

[3] R. Bernewitz, G. Guthausen, H. P. Schuchmann, Magn. Reson. Chem. 49 (2011) S93-S104. DOI: 10.1002/mrc.2825

[4] R. Bernewitz, U. S. Schmidt, H. P. Schuchmann, G. Guthausen (2014). Colloids Surf. A: Physicochem. Eng. Aspects 458 (2014) 10-18. DOI: 10.1016/j.colsurfa.2014.01.002

[5] P. S. Denkova, S. Tcholakova, N. D. Denkov, K. D. Danov, B. Campbell, C. Shawl, D. Kim, Langmuir 20 (2004) 11402-11413. DOI: 10.1021/la048649v

[6] F. Wolf, L. Hecht, H. P. Schuchmann, E. H. Hardy, G. Guthausen, Eur. J. Lipid Sci. Tech. 111 (2009) 730-742. DOI: 10.1002/ejlt.200800272

[7] X. Guan, K. Hailu, G. Guthausen, F. Wolf, R. Bernewitz, H. P. Schuchmann, Eur. J. Lipid Sci. Tech. 112 (2010) 828–837. DOI: 10.1002/ejlt.201000022

[8] L. Vermeir, P. Sabatino, M. Balcaen, A. Declerck, Dewettinck K., J. C. Martins, P. Van der Meeren, J. Colloid Interface Sci. 463 (2016) 128-136. DOI: 10.106/j.jcis.2015.10.023

[9] J. S. Murday, R. M. Cotts, J. Chem. Phys. 48 (1968) 4938-4945. DOI: 10.1063/1.1668160

[10] J. P. Hindmarsh, J. Su, J. Flanagan, H. Singh, Langmuir 21 (2005) 9076-9084. DOI: 10.1021/la051626b

[11] L. Vermeir, M. Balcaen, P. Sabatino, K. Dewettinck, P. Van der Meeren, Colloids Surf. A: Physicochem. Eng. Aspects 456 (2014) 129–138. DOI: 10.1016/j.colsurfa.2014.05.022

[12] B. Balinov, P. Linse, O. Söderman, J. Colloid Interface Sci. 182 (1996) 539-548. DOI: 10.1006/jcis.1996.0498

[13] I. Fourel, J. P. Guillement, D. Le Botlan, J. Colloid Interface Sci. 164 (1994) 48-53. DOI: 10.1006/jcis.1994.1142

[14] J. C. Van den Enden, D. Waddington, H. van Aalst, C. G. Van Kralingen, K. J. Packer, J. Colloid Interface Sci. 140 (1990) 105-113. DOI: 10.1016/0021-9797(90)90327-K

[15] J. Pfeuffer, U. Flögel, W. Dreher, D. Leibfritz, NMR Biomed. 11 (1998) 19-31. DOI:

10.1002/(SICI)1099-1492(199802)11:1<19::AID-NBM499>3.0.CO;2-O

[16] R. Mezzenga, Food Hydrocoll. 21 (2007) 674–682. DOI: 10.1016/j.foodhyd.2006.08.019

[17] S. Lasič, I. Åslund, D. Topgaard, J. Magn. Reson. 199 (2009) 166–172. DOI: 10.1016/j.jmr.2009.04.014

[18] N. N. Yadav, W. S. Price, J. Colloid Interface Sci. 338 (2009) 163-168. DOI: 10.1016/j.jcis.2009.06.014

[19] C. Malmborg, D. Topgaard, O. Söderman, J. Colloid Interface Sci. 263 (2003) 270–276. DOI: 10.1016/S0021-9797(03)00259-5

[20] J. Su, J. Flanagan, Y. Hemar, H. Singh, Food Hydrocoll. 20 (2006) 261-268. DOI: 10.1016/j.foodhyd.2004.03.010

[21] J. P. M. van Duynhoven, B. Maillet, J. Schell, M. Tronquet, G. J. W. Goudappel, E. Trezza, A. Bulbarello, D. van Dusschoten, Eur. J. Lipid Sci. Tech. 109 (2007) 1095–1103. DOI: 10.1002/ejlt.200700019

[22] H. J. Motulsky, L. A. Ransnas, FASEB J. 1 (1987) 365–374.

[23] M. L. Johns, Curr. Opin. Colloid Interface Sci. 14 (2009) 178–183.

[24] M. A. Voda, J. P. M. van Duynhoven, Trends Food Sci. Tech. 20 (2009) 533-543. DOI: 10.1016/j.tifs.2009.07.001

[25] K. J. Packer, C. J. Rees, J. Colloid Interface Sci. 40 (1972) 2, 216-218.

[26] S. M. Schoberth, N.-K. Bär, R. Krämer, J. Kärger, Anal. Biochem. 279 (2000) 100-105. DOI: 10.1006/abio.1999.4450

[27] S. So, T. P. Lodge, J. Phys. Chem. C 118 (2014) 21140-21147. DOI: 10.1021/jp50518h

[28] J. Cheng, J.-F. Chen, M. Zhao, Q. Luo, L. Wen, K. D. Papadopoulos, J. Colloid Interface Sci. 305 (2007) 175-182. DOI: 10.1016/j.jcis.2006.09.055

[29] M. H. Hilder, JAOCS 45 (1968) 703-707. DOI: 10.1007/BF02541262

[30] M. H. Hilder, M. van den Tempel, J. Appl. Chem. Biotechn. 21 (1971) 176-179.

[31] M. L. Johns, K. G. Hollingsworth, Prog. Nucl. Mag. Res. Sp. 50 (2007) 51–70. DOI: 10.1016/j.pnmrs.2006.11.001

[32] S. Kiokias, A. A. Reszka, A. Bot, Int. Dairy J. 14 (2004) 287-295. DOI: 10.1016/j.idairyj.2003.09.007

[33] A. Einstein, Annalen der Physik 17 (1905) 549-560.

[34] L. M. Diamante, T. Lan, J. Food Processing (2014) 1-6. DOI: 10.1155/2014/234583

[35] L. Wen, K. D. Papadopoulos, Colloids Surf. A: Physicochem. Eng. Aspects 174 (2000) 159-167. DOI: 10.106/S0927-7757(00)00508-2

Figure captions

Fig. 1. Schematically drawn systems. (a) W/O/W emulsion with negligible exchange between the inner water droplets, as well as between the inner water droplets and the external water phase. (b) W/O/W emulsion with negligible exchange between the inner (p_1) and outer water phase (p_3) and mean residence time τ_1 and τ_2 in p_1 (W_1) and p_2 (oil), respectively.

Fig. 2. (a) Simulated normalized echo decay of a W/O/W emulsion (and inset at small q^2) using Eq. (3), $D_2 = 1.1 \times 10^{-9}$ m^2/s, $p_2 = 0.75$, $\tau_1 = 0.1$ s (– · –) for $\Delta = 140$ ms (grey) and $\Delta = 220$ ms (black). Using Eq. (4), with EV = 25%, $D_2 = 0.4 \times 10^{-9}$ m^2/s, $p_2 = 0.01$ and $D_3 = 1.1 \times 10^{-9}$ m^2/s, the following echo decays were simulated for $\tau_1 = 0.1$ s (—) and $\Delta = 60$ ms (light grey), $\Delta = 140$ ms (grey) and $\Delta = 220$ ms (black); $\tau_1 = 30$ s and $\Delta = 60$ ms (– –); $\tau_1 = 30$ s and $\Delta = 220$ ms (···). For both equations, the values of δ, R_{43}, σ, and I_0 were set at 2.5 ms, 1.50 µm, 0.25 µm and 1, respectively. (b) Experimentally obtained normalized echo decay of the sodium caseinate stabilized W/O$_s$/W emulsion as measured at 35 °C using low-resolution NMR. Full lines represent the fitting of Eq. (4) to the experimentally obtained diffusion data at a diffusion delay Δ (60-140-220 ms).

Fig. 3. Normalized echo intensity of water (triangles) and TMACl (squares) in the W/O/W emulsion as measured at 5 °C using $\Delta = 600$ ms by high-resolution NMR. The lines represent the fitting of Eq. (1) to the diffusion data.

Fig. 4. Effect of diffusion delay value Δ (250-450-600 ms) on the normalized echo intensity of (a) water and (b) TMACl in the W/O/W emulsion as measured at 25 °C with high-resolution NMR. The lines represent the fitting of Eq. (1) to the diffusion data.

Fig. 5. Effect of measurement temperature and diffusion delay on the estimated R_{43}-value of the W/O/W emulsion as based on water (circles) and TMACl (diamonds) diffusion data using HR-NMR and $\Delta = 600$ ms (black filled markers), $\Delta = 450$ ms (grey filled markers) and $\Delta = 250$ ms (empty markers). Also the radius obtained from the LR-diffusion data at 600 ms (∗) is included. Lines represent a guide to the eye.

Fig. 6. Echo intensity of water in the W/O$_s$/W emulsion as measured at 5 °C (a) and 35 °C (b). Full lines represent the fitting of Eq. (1), whereas the dashed-dotted lines refer to the fitting using Eq. (4) to the experimentally obtained diffusion data (markers) at a diffusion delay Δ of 60 ms (diamonds), 80 ms (crosses), 100 ms (triangles), 140 ms (circles) and 220 ms (squares).

Fig. 7. Effect of measurement temperature and diffusion delay Δ on the estimated R_{43}-value upon fit of Eq. (1) (solid markers) or Eq. (4) (empty circles) to the water diffusion data of the (a) $W/O_s/W$ emulsion and (b) $W/O_h/W$ emulsion using LR-NMR. Einstein's diffusion law fit of Eq. (5) (crosses) to the fitted results from Eq. (1) are also included. Dotted lines represent a guide to the eye.

Fig. 8.

Fit of Einstein's diffusion law using Eq. (5) (lines) to the apparent water droplet radius R_{43} of the $W/O_h/W$ emulsion as obtained from Eq. (1) (markers) using different Δ values and temperatures.

Table 1

Best fitted values for the residence time of water molecules within the internal water droplets (τ_1) for the W/O/W emulsion using Eq. (4).

	τ_1 (s)	
T (°C)	W/O_s/W	W/O_h/W
5	1.00 ± 0.27	1.57 ± 2.61
15	0.79 ± 0.16	0.44 ± 2.80
25	0.33 ± 0.14	0.56 ± 0.23
35	0.09 ± 0.09	0.30 ± 0.11

Table 2

Output of Einstein's diffusion law fit (Eq. (5)) to the R_{43}-values of the W/O/W emulsion as obtained from Eq. (1). Questionable fitting of the $W/O_s/W$ data at 25 °C are placed between brackets.

	$R_{43,0}$ (μm)		D (10^{-11} m^2/s)	
T (°C)	$W/O_s/W$	$W/O_h/W$	$W/O_s/W$	$W/O_h/W$
5	0.92 ± 0.13	2.03 ± 0.13	0.11 ± 0.11	0.01 ± 0.02
15	1.10 ± 0.08	1.96 ± 0.17	0.14 ± 0.05	0.05 ± 0.08
25	(2.76 ± 0.24)	2.06 ± 0.14	(0.06 ± 0.11)	0.13 ± 0.10
35	1.35 ± 0.10	1.91 ± 0.22	1.72 ± 0.29	0.65 ± 0.41

Graphical abstract

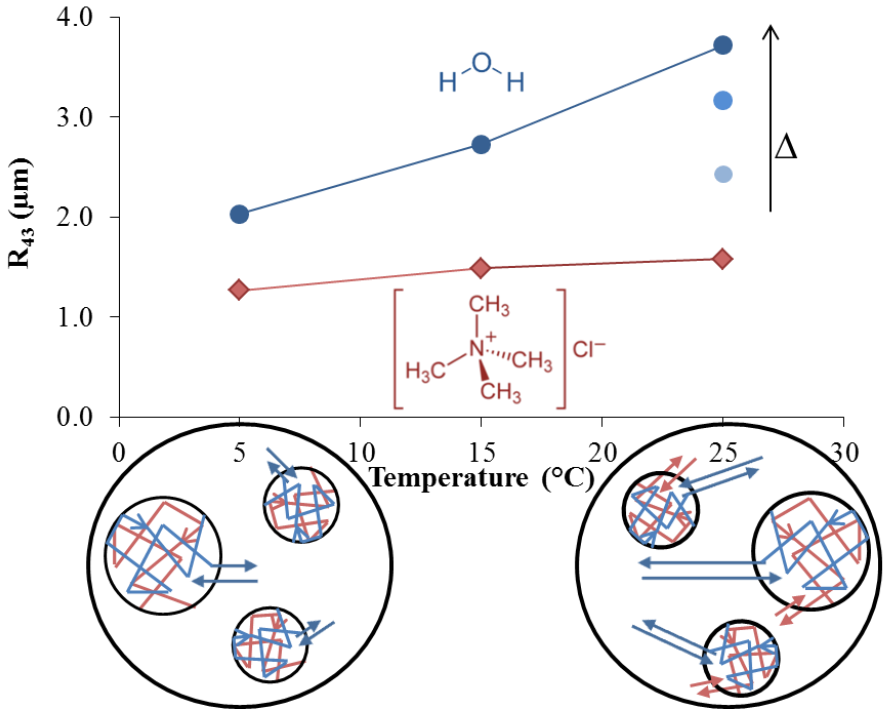

Title:

Effect of molecular exchange on water droplet size analysis as determined by diffusion NMR: the W/O/W double emulsion case

Abbreviations in the Title

NMR, Nuclear Magnetic Resonance; W/O/W, water-in-oil-in-water

Authors names and affiliations:

Lien Vermeir[a*], Paolo Sabatino[a,b], Mathieu Balcaen[a], Arnout Declerck[a], Koen Dewettinck[c], José C. Martins[b], Gisela Guthausen[d] and Paul Van der Meeren[a]

("Van der Meeren" is the family name of author Paul Van der Meeren, the family names of the other authors are their last names as appear above)

[a] Particle and Interfacial Technology Group, Department of Applied Analytical and Physical Chemistry, Faculty of Bioscience Engineering, Ghent University, Coupure Links 653, B-9000 Ghent, Belgium

[b] NMR and Structure Analysis Unit, Department of Organic Chemistry, Faculty of Sciences, Ghent University, Krijgslaan 281 S4, B-9000 Ghent, Belgium

[c] Laboratory of Food Technology and Engineering, Department of Food Safety and Food Quality, Faculty of Bioscience Engineering, Ghent University, Coupure Links 653, B-9000 Ghent, Belgium

[d] Pro^{2}NMR, MVM and IBG-4, Karlsruher Institut für Technologie, Adenauerring 20b, DE-76131 Karlsruhe, Germany

Lien.Vermeir@UGent.be, P.Sabatino@yahoo.it, Mathieu.Balcaen@UGent.be, Arnout.Declerck@UGent.be, Koen.Dewettinck@UGent.be, Jose.Martins@UGent.be, Gisela.Guthausen@kit.edu, Paul.VanderMeeren@UGent.be

[*]**Corresponding author**. Particle and Interfacial Technology Group, Faculty of Bioscience Engineering, Ghent University, Coupure Links 653, B-9000 Ghent, Belgium. Tel.: +32 9 264 99 06. Email address: Lien.Vermeir@UGent.be

Abstract

Hypothesis

The accuracy of the inner water droplet size determination of W/O/W emulsions upon water diffusion measurement by diffusion NMR was evaluated. The resulting droplet size data were compared to the results acquired from the diffusion measurement of a highly water soluble marker compound with low permeability in the oil layer of a W/O/W emulsion, which provide a closer representation of the actual droplet size. Differences in droplet size data obtained from water and the marker were ascribed to extra-droplet water diffusion.

Experiments

The diffusion data of the tetramethylammonium cation marker were measured using high-resolution pulsed field gradient NMR, whereas the water diffusion was measured using both low-resolution and high-resolution NMR. Different data analysis procedures were evaluated to correct for the effect of extra-droplet water diffusion on the accuracy of water droplet size analysis.

Findings

Using the water diffusion data, the use of a low measurement temperature and diffusion delay Δ could reduce the droplet size overestimation resulting from extra-droplet water diffusion, but this undesirable effect was inevitable. Detailed analysis of the diffusion data revealed that the extra-droplet diffusion effect was due to an exchange between the inner water phase and the oil phase, rather than by exchange between the internal and external aqueous phase. A promising data analysis procedure for retrieving reliable size data consisted of the application of Einstein's diffusion law to the experimentally determined diffusion distances. This simple procedure allowed determining the inner water droplet size of W/O/W emulsions upon measurement of water diffusion by low-resolution NMR at or even above room temperature.

Keywords: molecular exchange; water exchange; tetramethylammonium chloride; water droplet size analysis; W/O/W emulsion (water-in-oil-in-water); diffusion NMR (Nuclear Magnetic Resonance); pfg-NMR diffusometry (pulsed field gradient); low-resolution NMR; high-resolution NMR

Abbreviation in the text[1]

[1] NMR, Nuclear Magnetic Resonance; pfg, pulsed field gradient; W/O/W, water-in-oil-in-water; TMACl, tetramethylammonium chloride

1. Introduction

Water-in-oil-in-water (W/O/W) emulsions have the potential to create light foods as part of the oily dispersed phase is replaced by water [1]. In order to optimize the double emulsion formulation and to control its stability and functionality, the inner water droplet size distribution and internal water fraction can be determined. A wide range of emulsions in food process control and development have been characterized by low-resolution benchtop NMR [2]. The droplet size distribution of O/W, W/O, W/O/W and O/W/O emulsions can be determined using ^{1}H pulsed field gradient (pfg) NMR diffusometry [3-8]. Hereby, the droplet size distribution is estimated upon measurement of the restricted (intra-droplet) diffusion coefficient of molecules of the dispersed phase, followed by data analysis such as the procedure described by Murday and Cotts [9]. The latter procedure assumes that the droplet boundaries are impermeable. In addition, low-resolution NMR has also been applied to obtain information about the inner water volume fraction of W/O/W emulsions [6,10,11].

We have recently shown that molecular transport of water molecules through the oil layer of water-in-oil (W/O) emulsions can be detected using diffusion NMR [8]. This type of extra-droplet water diffusion was shown to become more important when raising the measurement temperature and NMR diffusion delay time Δ [6,8,12-14]. Extra-droplet water diffusion brought about an apparent increase in mean droplet size of W/O emulsions when using the Murday and Cotts data procedure [9], as well as when using the available data procedure that takes exchange into account [15]. These artefacts were unavoidable even when performing the diffusion analysis at low Δ and temperature. A data splicing procedure and the use of Einstein's diffusion law were proposed for determination of the droplet size, minimally affected by water exchange [8].

As W/O/W emulsions are more complex systems, it is interesting to evaluate whether the above mentioned instructs (i.e. low Δ and temperature) for minimizing the effect of extra-droplet water diffusion on the accuracy of water droplet size analysis also apply for W/O/W emulsions. For the same purpose, different data analysis procedures were evaluated. As a solid crystalline fat might suppress diffusion processes of water through the fat phase layer [16], the double emulsions were prepared either using a liquid oil or a solid fat.

To that end, both high-resolution NMR and low-resolution NMR, a more practical approach for measuring water diffusion, were applied. The former method enables the measurement of the spectrally-resolved diffusion signal of aqueous dissolved molecular species and water molecules in the water phases of W/O/W emulsions. Synchronous analysis of both signals allows the verification of the occurrence of molecular exchange. The water soluble tetramethylammonium chloride was selected, on account of an intense signal in a specific NMR region without overlap with water or oil, in addition to its low permeability through the oil phase due to its ionic nature [8,17-19].

To the best of our knowledge, this is the first simultaneous multi-nuclear temperature dependent diffusion analysis of water and a dissolved marker enclosed in W/O/W emulsion droplets as measured at different diffusion delays Δ using low-resolution and high-resolution pfg-NMR.

2. Materials and methods

2.1. Materials

The lipophilic emulsifier polyglycerol polyricinoleate (PGPR 4150; min. 75% n-glycerols with n = 2, 3 and 4; max. 10% m-glycerols with m $\geq$ 7) was kindly provided by Palsgaard A/S (Denmark). The hydrophilic emulsifier sodium caseinate (5.5% moisture; 96% protein on dry matter) was received as a gift sample from Armor Protéines (Saint Brice en Cogles, France), whereas Polysorbate 80 (Tween 80) was obtained from Sigma-Aldrich (Steinheim, Germany). High oleic sunflower oil (Hoso, Iodine Value = 87; 82% C18:1; SFC = 0% at 5 °C) was acquired from Contined B.V. (Bennekom, The Netherlands). Soft palm mid fraction (soft PMF; Iodine Value = 42-50; SFC = 79% at 5 °C) was purchased from Unigra Sp. (Conselice, Italy).

Tetramethylammonium chloride (TMACl, 109.6 g/mol) was obtained from Sigma-Aldrich (Steinheim, Germany). Deuterated water with a purity of 99.8 atom %D was purchased from Armar Chemicals (Switzerland). Food grade xanthan gum (FF) was a generous gift sample from Jungbunzlauer (Vienna, Austria). The 0.1 M phosphate buffer solution (pH 6.7) contained 0.02% (w/v) of the anti-microbial agent NaN_3 (Acros Organics, Geel, Belgium), KH_2PO_4 (Merck KGaA, Darmstadt, Germany) and K_2HPO_4 (Alfa Aesar, Karlsruhe, Germany). Unless stated differently, the above mentioned chemicals were of analytical grade.

2.2. Sample preparation

The inner (W_1) and outer (W_2) water phase of the $W_1/O/W_2$ emulsions that were investigated by both high and low-resolution NMR contained 800 mM TMACl in a mixture of D_2O/H_2O (50:50, wt%). In addition, the W_2 phase contained 0.2 wt% xanthan gum and 1.4 wt% Tween 80. The oil phase consisted of 2.5 wt% PGPR in Hoso. The W_1/O emulsions (40 g of 50:50, w/w) were mixed at 60 °C with an Ultra-Turrax (type S25KV - 25G, IKA®-Werke, Germany) at 6500 rpm for 4 min. The $W_1/O/W_2$ (30 g of 20:20:60, w/w) was prepared at room temperature upon mixing the W_1/O emulsion with W_2 phase with an Ultra-Turrax (type S25-10G, IKA®-Werke, Germany) at 9500 rpm for 1 min.

Regarding the composition of emulsions investigated only by low-resolution NMR, reference is made to the procedure described by Su et al. [20], which differs in the applied phase ratio and surfactant concentration. An Ultra-Turrax (type S 50 N - G 45 F, IKA®-Werke, Germany) and a Microfluidizer (type

M110S, Microfluidics) at 840 bar (driving air pressure of 6 bar) for 1.5 min were used to premix and homogenize the W_1/O emulsion (160 g, 50:50, w/w) at 60 °C, respectively. The primary water phase (W_1) contained 1.25% (w/v) sodium caseinate and 0.1 M phosphate buffer solution, whereas the fat phase consisted of 2.5% (w/v) PGPR in soft PMF or Hoso. The $W_1/O/W_2$ (100 g) emulsion was prepared at room temperature upon mixing the external water phase (W_2) with freshly prepared W_1/O emulsion in a 60:40 (w/w) ratio with an Ultra-Turrax S25-10G (IKA®-Werke, Germany) at 13500 rpm for 1 minute. Hereby, the W_2 phase only differs from the W_1 phase in the concentration of sodium caseinate (1%, w/v). Afterwards, all double emulsions were further mixed with a continuous Ultra-Turrax DK25 (IKA®-Werke, Germany) at 13500 rpm for 1 minute.

All samples were cooled in an ice/water bath for 40 minutes and subsequently stored in the refrigerator.

2.3. High-resolution NMR

High-resolution pfg-NMR diffusion analysis was performed with a Bruker Avance III spectrometer operating at a ^1H frequency of 500.13 MHz and equipped with a 5 mm DIFF30 gradient probe with a maximum gradient strength of 18 T/m. Measurements were performed at 5, 15 or 25 °C and the temperature was controlled to within ± 0.01 °C with a Eurotherm 3000 VT digital controller. The samples (560 to 650 µL) were filled in 5 mm diameter glass NMR-tubes (Armar Chemicals, Switzerland). Pulsed field gradient (pfg) NMR experiments were performed using the conventional single stimulated echo pulse sequence. The applied δ and Δ for the Tween 80-stabilized W/O/W emulsion was 4.5 ms and 250-450-600 ms, respectively. The free self-diffusion coefficient of water and TMACl in the water phase (W_1) was measured (D_s) upon varying G between 0.03 and 1.3 T/m while keeping δ and Δ constant at 1 ms and 50 ms, respectively ($D_{s,\,water}$ = 1.14 x 10^{-9}, 1.53 x 10^{-9} and 2.00 x 10^{-9} m^2/s at 5, 15 and 25 °C and $D_{s,\,TMACl}$ = 5.10 x 10^{-10}, 7.03 x 10^{-10} and 9.01 x 10^{-10} m^2/s, respectively).

2.4. Low-resolution NMR

NMR measurements were performed on a benchtop Maran Ultra spectrometer (Oxford Instruments, UK) operating at a frequency of 23.4 MHz. The samples were adequately filled [11] in 18 mm diameter glass NMR-tubes (Oxford Instruments, UK). Pulsed field gradient (pfg) NMR experiments were performed using the stimulated echo pulse (STE) sequence, which was preceded by an inversion recovery experiment for suppression of the NMR-signal from the fat phase in the emulsion, characterized by a time period τ_{null} [2]. Measurements were performed varying the gradient strength (G) [21] between 0 and 3.17 T/m. The applied δ and Δ for the experiment on sodium caseinate stabilized W/O/W emulsions was 2.5 ms and 60-80-100-140-220 ms, respectively. In order to enable comparison with the high-resolution NMR experiment, higher values of δ and Δ were applied for the measurement of the Tween 80-stabilized

W/O/W emulsions, i.e. 4.5 ms and 240-440-600 ms, respectively. For the other applied NMR parameters we refer to [11]. The free self-diffusion coefficient of the water phases was measured (D_s) using the DSD script (Oxford Instruments, UK) and varying δ between 0.05 and 2.75 ms while keeping G and Δ constant at 0.14 T/m and 200 ms, respectively. The D_s of the W_1 phase containing 1.25% sodium caseinate in 0.1 M phosphate buffer solution amounted to 1.20 x 10^{-9}, 1.75 x 10^{-9}, 2.29 x 10^{-9} and 2.82 x 10^{-9} m^2/s at 5, 15, 25 and 35 °C, respectively. The D_s values of the 800 mM TMACl containing W_1 phase amounted to 8.82 x 10^{-10}, 1.23 x 10^{-9} and 1.58 x 10^{-9} m^2/s at 5, 15 and 25 °C. These values roughly comply with the weighted average of the $D_{s,\,water}$ and $D_{s,\,TMACl}$ as obtained from high-resolution NMR. Using a H-molar concentration for H_2O of 55.6 mol H per liter (i.e. ½ x 55.6 mol/L x 2 mol H/mol), a H-molar concentration for TMACl of 9.6 mol H per liter (i.e. 0.8 mol/L x 12 mol H/mol) and a fraction for water of 55.6/(55.6+9.6), the weighted average amounts to 1.05 x 10^{-9}, 1.41 x 10^{-9} and 1.84 x 10^{-9} m^2/s at 5, 15 and 25 °C, respectively.

2.5. Statistical analysis

Unless stated differently, the uncertainty of the estimated values and error bars in the graphs represent the standard error of the estimates. The latter values were obtained directly from the Matlab fitting procedure, by the Monte Carlo method [22] or by linear regression in Excel (Microsoft Office 2010), from which a 95% confidence interval could be constructed. Regarding the comparison of model fitting with a different number of parameters of the diffusion data, the applied measure of goodness-of-fit was the root mean squared error (RMSE), whereas the fit to relative trend was measured by the adjusted R^2-value.

3. Background theory

Differences in diffusion behavior in W/O/W emulsions allow discriminating between internal and external water. Water molecules in the external water phase experience quasi free diffusion ('FW') (with a minor obstruction effect due the oil globules present) characterized by D_e, whereas the diffusion in the internal water droplets is restricted. The latter can be described by the Murday and Cotts equation E_{MC} [9,23,24], assuming that the diffusion of the inner water droplets, as well as the water exchange through the oil or fat phase is negligible during the analysis (Fig. 1a). A full expression of E_{MC} can be found in [24].

Provided that the two water compartments can be regarded as independent [11], a combination of fast and slow echo decay is recorded at low and high values of q^2, respectively, and the water signal should give rise to a quasi bi-component decay E_{MCFW} (Eq. (1)) as a function of q^2 and diffusion delay Δ.

$$E_{MCFW}(q^2,\Delta) = \frac{I}{I_0} = EV \cdot \frac{\int_0^\infty P_v(R) \cdot E_{MC}(R,q^2,\Delta)dR}{\int_0^\infty P_v(R)\,dR} + (1-EV)\cdot \exp\left(-q^2 \cdot \left(\Delta - \frac{\delta}{3}\right) \cdot D_e\right) \qquad (1)$$

The amplitudes of the echo decay yield the enclosed water volume fraction, which is the fraction of the total water that is present as internal water droplets. To account for polydisperse droplet sizes, the normalized attenuation of the NMR signal I/I_0 of the population of possible spherical droplet radii R with a certain probability P_v can be described by the first term in Eq. (1) [3,24,25]. Hereby, P_v is usually modelled by a lognormal volume-weighted particle size distribution (Eq. (2a)), I_0 is the echo intensity in the absence of a magnetic field and q is a function of the gyromagnetic ratio γ (2.675 x 10^8 s^{-1} T^{-1}), the gradient duration δ and the gradient strength G according to $q^2 = (\delta \cdot \gamma \cdot G)^2$. The geometric mean radius (R_{33}) and geometric standard deviation (σ_g) in Eq. (2a) were converted to the arithmetic mean radius (R_{43}) and arithmetic standard deviation (σ) of the lognormal volume-weighted particle size distribution using Eqs. (2b,c).

$$P_v(R) = \frac{1}{\sqrt{2\pi}\cdot R \cdot \ln\,\sigma_g} \cdot \exp\left(-\frac{\left(ln(R) - ln(R_{33})\right)^2}{2\cdot\left(\ln\,\sigma_g\right)^2}\right) \tag{2a}$$

$$R_{43} = R_{33} \cdot \exp\left(\frac{\left(\ln\,\sigma_g\right)^2}{2}\right) \tag{2b}$$

$$\sigma = \sqrt{R_{43}^2 \cdot \left(exp\left(\left(\ln\,\sigma_g\right)^2\right) - 1\right)} \tag{2c}$$

The values for EV, R_{43}, I_0 and the effective diffusion coefficient in the outer aqueous phase (D_e) were determined upon performing a least-squares fit of Eq. (1) to the echo intensity data as measured for a certain Δ using Matlab 7.5.0.342 (R2007b) software (The MathWorks). For reasons of unreliable estimations, the arithmetic standard deviation σ was estimated upon fitting the first term of Eq. (1) (with EV = 100%) to the echo decay of the associated primary W/O emulsion; the best fitted σ-values are mentioned in [8].

In case that exchange occurs between two compartments, the exchange model as described by Pfeuffer et al. [15] and Schoberth et al. [26] can accommodate the diffusion behavior of water in the inner compartment, with finite water permeability, surrounded by external water:

$$E_{Pf}(q^2,\Delta) = p_1' \cdot \exp\left(-q^2 \cdot \left(\Delta - \frac{\delta}{3}\right) \cdot D_1'\right) + p_2' \cdot \exp\left(-q^2 \cdot \left(\Delta - \frac{\delta}{3}\right) \cdot D_2'\right) \tag{3}$$

Prime symbols indicate the parameters influenced by exchange of molecules and are henceforth termed apparent parameters. As such, the amplitudes and slopes of the echo decay will yield apparent water volume fractions ($p_{1,2}'$) and apparent diffusion coefficients of the inner and outer compartments ($D_{1,2}'$), which are functions of their real values ($p_{1,2}$ and $D_{1,2}$) and the mean residence time ($\tau_{1,2}$) in the internal and external water pool [8]. Hereby, D_1 (and the inner compartmental size distribution) results from taking

the partial derivative of the first term of Eq. (1) with respect to q^2. Consequently, molecular exchange can be observed when D_1 and D_2 differ and the concentrations in both compartments and of exchanging molecules are large enough.

4. Results and discussion

4.1. Exchange model selection

In literature, the exchange model (Eq. (3)) has been applied to describe the diffusion signal of water exchanging between the two water phases of a W/O/W emulsion [10]. Assuming that the volume fraction of water in oil can be considered negligible [7], the values of $p_{1,2}$, $p'_{1,2}$, $D_{1,2}$, $D'_{1,2}$ and $\tau_{1,2}$ are associated with the inner and outer water pool. Simulation of the normalized NMR echo decay as a function of q^2 using Eq. (3) is shown in Fig. 2a. The simulated echo decay is characterized by two slopes, a larger slope at low q^2 and a smaller slope at large q^2 values. The slope of the fast decaying part increases for increasing Δ, whereas the slope of the slower part remains constant, but its amplitude decreases as attributed to extra-droplet diffusion of water through the oil layer inside the multiple droplets, as well as between the inner and outer water compartment. This statement is valid as long as there is exchange between the two water phases during the diffusion time Δ (dashed-dotted lines in Fig. 2a).

The simulated signal decays strongly change when water exchange between the two water phases is negligible during Δ, but primarily occurs between the inner water droplets and the oil phase (full lines in Fig. 2a). The extrapolated value for $q \rightarrow 0$ reflects the relative amplitudes of inner and outer water phases which should be independent of the values of the experimental NMR parameters. The NMR attenuation data of the double emulsions in our study exhibited the expected distinct echo decays. Fig. 2b shows that the slope of the slowly decreasing part of the echo decay of the sodium caseinate stabilized double emulsion as measured at 35 °C increased as the diffusion delay was increased and showed a common intercept. The former points to considerable extra-droplet exchange inside the multiple droplets, whereas the latter indicates that the exchange between the inner and outer water compartment was negligible within the time frame considered (i.e. two independent water compartments). Moreover, it suggests that the amplitudes of the echo decay related to the real enclosed water volume fraction remain constant over time, i.e. the molecular exchange is a phenomenon in a stable emulsion.

When neglecting the size distribution, the slope at high q^2 values indicate the droplet size. Hereby, the slope (and 95% confidence interval) of this slowly decreasing part amounted to -0.8 ± 0.1, -1.3 ± 0.1 and -1.8 ± 0.1 μm^2 at Δ of 60, 140 and 220 ms, whereas the slope of the fast decaying part amounted to -83 ± 13, -93 ± 48 and -93 ± 69 μm^2, respectively.

Upon extending the exchange model with a free water diffusion term, all three phases are considered, i.e. water molecules in the inner and outer water phases as well as in the oil phase. This extended model was able to fit the experimentally obtained echo decays in Fig. 2b:

$$E(q^2,\Delta) = \frac{I}{I_0} = EV \cdot E_{Pf}(q^2,\Delta) + (1 - EV) \cdot \exp\left(-q^2 \cdot \left(\Delta - \frac{\delta}{3}\right) \cdot D_3\right) \quad (4)$$

The first term of Eq. (4) contains the parameters influenced by exchange between water droplets (1st pool) and the oil layer (2nd pool) inside the oil droplets of the W/O/W emulsion, whereas the second term yields the effective diffusion coefficient D_3 of the external water phase (3rd pool), similar to D_e in Eq. (1). A schematic representation of Eq. (4) and its simulated diffusion echo signal decays are given in Fig. 1b and Fig. 2a, respectively.

The values of R_{43}, σ, τ_1, p_2, I_0, D_2, EV and D_3 were determined upon performing a least-squares fit of Eq. (4) to the echo intensity data as measured for a series of Δ using Matlab 7.5.0.342 (R2007b) software (The MathWorks). The water volume fraction in the inner water phase (p_1) and the mean residence time of water in the oil layer (τ_2) follow from $p_1 = 1 - p_2$ and $\tau_2 = \tau_1 \cdot \frac{1-p_1}{p_1}$, respectively. D_1 as a function of q^2 results from taking the partial derivative of the first term of Eq. (1) with respect to q^2 using the estimated R_{43} and σ.

In other studies [6,10], Eq. (3) was applied to fit the diffusion data of W/O/W emulsions to describe the exchange between internal and external water. The requirement of an extension of the exchange model (Eq. (4)) in which only exchange between the internal water and the oil phase is considered is explained by our different experimental settings and emulsion recipe as compared to others [6,10]. It is widely known that the double emulsion characteristics, and hence its diffusion signals, are strongly affected by the actual emulsion composition and preparation method. In our case, the 20:20:60 W/O/W emulsions with an external water phase either containing sodium caseinate without xanthan, sodium caseinate with 0.2% xanthan (data not shown) or Tween 80 with 0.2% xanthan showed the features as shown in Fig. 2b, which according to simulation (Fig. 2a) results from exchange between the internal water and oil phase, rather than from exchange between internal and external water phase.

4.2. Water versus tetramethylammonium chloride diffusion

In order to confirm the interpretation of the signal decays in section 4.1 independently, a tracer diffusion study was performed additionally. To study the water and marker compound diffusion in W/O/W emulsions, low and high-resolution pfg-NMR diffusometry were applied. Low-resolution NMR predominantly measures the diffusion of water molecules, whereas high-resolution NMR enables separate diffusion analysis of all ingredients separately due to chemical shift dispersion. I.e. water and water

soluble compounds as well as oil can be analyzed separately. This opens interesting perspectives since water soluble ionic marker molecules have a reduced permeability in hydrophobic media as oil in comparison to water molecules [19,27]. Ion transport through the oil film in W/O/W emulsions was shown to be driven by the osmotic pressure gradient across the oil film. Without osmotic pressure, its transport became hardly observable [28]. Upon addition of tetramethylammonium chloride to the inner and outer water phase of the W/O/W emulsion at the same concentration, the resulting marker diffusion signal associated with the inner water compartment is expected to reflect the maximum travelled distance that is Δ-independent and only affected by the droplet size, shape and compartmental water fractions, provided that the diffusion delay value is sufficiently long [18,19].

4.2.1. High-resolution NMR of Tween 80-stabilized W/O/W emulsions

The measured NMR echo decays of water and TMACl of the W/O/W emulsion at 5 °C are shown in Fig. 3. Upon fitting of Eq. (1) to the water and marker diffusion signals, markedly different estimated water droplet size values are obtained. The best fitted R_{43}-value (with 95% confidence) amounted to 2.03 ± 0.04 µm and 1.27 ± 0.08 µm, respectively. The estimated enclosed water volume fraction amounted to 32 ± 1% and 29 ± 4%, respectively.

The effect of diffusion delay (250-450-600 ms) on the NMR echo decay of the W/O/W emulsion at 25 °C is shown in Fig. 4. The curves in Fig. 4a show a continuous increase in slope for $q \rightarrow 0$. Considering a q^2 range of up to 20 x 10^{12} m^{-2}, the diffusion data of the marker in Fig. 4b were less affected by Δ.

The best fitted R_{43}-values of the inner water droplets of the double emulsion are given in Fig. 5, which were similar to the values as obtained upon fitting Eq. (1) to the echo decay while neglecting the first few points at very small q^2. This further sustains the argument of independent water compartments. A much larger apparent increase in R_{43}-value with increasing temperature and/or Δ was observed for water than for the marker (Fig. 5). Two different types of diffusion might result in an apparent increase in droplet size, i.e. extra-droplet water diffusion (either by molecular transport or surfactant facilitated diffusion) as well as diffusion of the water droplets themselves by thermal agitation [24]. In fact, droplet movement by thermal agitation is expected to influence both sets of estimated radii as obtained from the water and TMACl diffusion data in the same way. As the water diffusion data are clearly much more influenced by an increase in temperature in Fig. 5, it follows that the mechanism responsible for the observed apparent size increase is related to a finite permeability of the species through oil during Δ.

The temperature-induced increase originates from a more Gaussian diffusing signal following an increase in solubility and diffusivity of water through oil with measurement temperature [29,30]. In contrast, the permeability of ionic marker molecules is significantly lower as attributed to a reduced solubility in hydrophobic media [19,27].

In comparison to 25 °C and 15 °C, the overestimation of the droplet size using the water signal was decreased at 5 °C. The remaining difference of the radius based on the water and marker signal at 5 °C, however, designates that the use of a low temperature cannot avoid the effects of extra-droplet water diffusion on the estimated droplet size using the water signal.

The Δ-induced increase of the estimated droplet size can be ascribed to the magnifying effect of Δ on the diffusion signal when molecular exchange occurs [18,19,31]. Consequently, the overestimation of the water droplet size based on the water signal as measured at 25 °C was less pronounced when using lower Δ values. As the marker signal resulted in a much lower R_{43}-dependency of temperature and Δ, it is thought to approximate the real water droplet radius.

4.2.2. Low-resolution NMR of Tween 80-stabilized W/O/W emulsions

Low-resolution NMR was applied on the W/O/W emulsion as a function of temperature at Δ = 600 ms (Fig. 5). The water signal resulted in the same trend of the estimated R_{43}-value as a function of temperature as in the HR-NMR experiment. It is worth mentioning that the complete sample volume was detected using low-resolution NMR. Therefore, the amplitudes of the fitting of Eq. (1) to the LR-NMR echo decay were used to estimate the EV. The EV was hardly affected by the measurement temperature (5-15-25 °C) using a diffusion delay Δ of 600 ms, nor by diffusion delay Δ (240-440-600 ms) at a temperature of 25 °C; all EV-values were in the range of 26.6 to 28.5%, with no significant effect of Δ and temperature. This observation further sustains the lack of exchange between the internal and external aqueous phase in our double emulsions, as was already claimed in section 4.1.

4.3. Water exchange modeling

To evaluate water exchange in W/O/W emulsions, different models were applied to fit the low-resolution NMR water diffusion data as measured at different diffusion delays and temperatures. Hereby, the objective was to perform accurate droplet size analysis, which requires disentanglement of the effect of water exchange on the best fitted values.

As a first procedure, the results of the application of a non-exchange (Eq. (1)) and exchange model (Eq. (4)) were compared. The soft PMF based ($W/O_s/W$) and the Hoso-based ($W/O_h/W$) samples, of which the outer interface was stabilized by sodium caseinate, as kept at 5 °C, were heated to 15, 25 and 35 °C. At each holding temperature, the diffusion data were recorded for Δ values between 60 and 220 ms. The fitting of Eq. (1) and Eq. (4) is shown for the $W/O_s/W$ emulsion in Fig. 6, for which the R^2_{adj} and RMSE amounted to at least 0.991 and at most 0.104 (at 5, 15 and 35 °C), except for the $W/O_s/W$ emulsion at 25 °C using Eq. (1), for which it amounted to 0.910 and 0.339, respectively. Hereby, the latter deviating

values are mainly due to the fitting results of the $W/O_s/W$ emulsion using Δ of 60 ms and 100 ms, for which larger uncertainties of the best fitted radius R_{43} are shown in Fig. 7a.

The best fitted radius R_{43} of the inner droplets of the W/O/W emulsions clearly increased with increasing measurement temperature, which became more obvious using larger Δ-values (Fig. 7). This effect might proceed from an increased water permeability through the oil, connected with an increased water saturation solubility and water diffusion coefficient in vegetable oil with increasing temperatures [29,30]. This was further evidenced by measurement of the emulsions upon cooling to 5 °C after previous measurements at higher temperatures. The droplet size of the cooled emulsions was comparable to the original non-heated sample; the sample averaged droplet size of the cooled $W/O_s/W$ and $W/O_h/W$ emulsion amounted to 1.11 ± 0.08 µm and 1.93 ± 0.05 µm, respectively. Therefore, the observed increase in droplet size at higher temperatures must originate from increased water exchange rather than a real temperature-induced increase in droplet size.

The results also indicate that an increased solid fat content (SFC) of the fat phase could not guarantee a less pronounced apparent droplet size increase. Hereby, the $W/O_s/W$ emulsion at the lowest temperatures (5 and 15 °C) is characterized by a very large viscosity due to the fat crystal network. In fact, the SFC of soft PMF at 5 and 15 °C amounted to 65% and 56%, whereas it amounted to 0% for Hoso oil as determined by pulsed NMR [11]. Based on the study of Kiokias et al. [32], diffusion of oil molecules in an oil phase with a SFC larger than 50% is restricted due to the fat network microstructure. Upon extrapolation towards W/O/W emulsions, it can be assumed that water droplets (much larger in size than oil molecules) in W/O/W emulsions with a SFC > 50% will also be largely restricted in their diffusion, if not completely immobilized in the solid fat matrix. As such, the apparent droplet size increase of the $W/O_s/W$ emulsion at low temperatures can only be explained by extra-droplet water diffusion.

The application of Eq. (4) resulted in a slightly less pronounced temperature effect on the best fitted radius of the W/O/W emulsion (Fig. 7). However, the extended exchange model could only partly compensate for the effect of exchange on the droplet size, despite that it is designed to take exchange into account. The residence times of water in the inner water compartment of the W/O/W emulsions in Table 1 decreased with increasing temperature. Similar to the primary W/O emulsions in [8], the water residence times measured at low sample temperature, as well as their estimation error, are much larger than the diffusion time, which indicates a small effect of water exchange on the droplet size.

Pertaining to the geometric standard deviation σ_g of the $W/O_h/W$ emulsions, the best fitted values using Eq. (4) were relatively temperature independent ($\sigma_g = 1.07 \pm 0.05$), unlike the $W/O_s/W$ emulsions, whose σ_g at 5 °C ($\sigma_g = 1.49$) and 15 °C ($\sigma_g = 1.38$) were larger than at 25 °C and 35 °C (for both $\sigma_g = 1.00$).

A second procedure was attempted to disentangle the estimated radius from the effect of exchange by means of a data splicing procedure. The procedure assumes that the diffusion data sets as measured at different temperatures and Δ originate from the same droplet size distribution. Upon jointly fitting the data to Eq. (4), a collective volume-weighted average droplet size is obtained, which amounted to 1.50 µm and 2.27 µm for W/O_s/W and W/O_h/W emulsion, respectively. As these values are significantly larger as compared to the experimental values obtained using Eq. (1) at low temperatures and low diffusion delay values, it follows that this procedure is not capable to completely eliminate extra-droplet water diffusion effects. Moreover, this data-splicing procedure has got the drawbacks to be complex, time-consuming and to hardly attach value to the data measured at higher temperature.

A third data analysis procedure to obtain a temperature independent radius assumes that the apparent increase in inner water droplet size is due to water diffusion through the oil phase. We have shown before that the distance travelled by diffusion in W/O emulsions could be corrected using Einstein's diffusion law (Eq. (5)) [33], which resulted in a diffusion delay independent droplet size ($R_{43,0}$), which is thought to approximate the real inner water droplet size [8].

$$R_{43}(T,\Delta) - R_{43,0}(T,\Delta = 0\ ms) = \sqrt{D(T)\cdot\Delta} \qquad (5)$$

In Fig. 8, a least-squares fit of Eq. (5) to the R_{43}-values of the W/O_h/W emulsion (as obtained from Eq. (1) at constant temperature) is presented. Table 2 indicates that the extrapolated intercept ($R_{43,0}$) is temperature independent. Fig. 7a shows the best fitted $R_{43,0}$-value of the W/O_s/W emulsion at 5 °C, which was about 0.3 µm smaller than the R_{43} obtained from Eq. (1) at Δ of 60 to 100 ms. The larger estimated radius $R_{43,0}$ and error margin at 25 °C are mainly due to the fitting results of the W/O_s/W emulsion using Δ of 60 ms and 100 ms. Fig. 7b includes the results for the W/O_h/W emulsion, for which the estimated radius $R_{43,0}$ was similar to the R_{43} obtained from Eq. (1) at 5 °C.

The best fitted diffusion coefficient values (D) mostly increased with increasing temperature according to an Arrhenius-type relationship (Table 2). Excluding the W/O_s/W data at 25 °C, the resulting activation energy (with 95% confidence) was E_a = 68 ± 267 kJ/mol (R^2 = 0.914), which was about 1.4 times smaller than for the W/O_h/W emulsion (E_a = 95 ± 32 kJ/mol, R^2 = 0.988). As a similar difference in E_a was previously noted between the W/O_s (Ea = 79 ± 14 kJ/mol, R^2 = 0.997) and W/O_h emulsion (Ea = 121 ± 88 kJ/mol, R^2 = 0.947) [8], the obtained values of D and E_a indicate that diffusion of water through the oil layer might depend on the fat phase composition.

The Stokes Einstein equation ($D = \frac{k_B \cdot T}{6 \cdot \pi \cdot \eta \cdot r}$ with the diffusion coefficient D of the sphere with effective hydrodynamic radius r, the dynamic viscosity of the surrounding fluid η and Boltzmann's constant k_B [33])

can be used to further elucidate the dominating type of diffusion related to the apparent increase in droplet size. As the volume-weighted average radius of the water droplets of the $W/O_h/W$ emulsion as measured at 25 °C amounted to 2.06 µm (Table 2), their diffusion coefficient in sunflower oil of 0.05 Pa·s at 298 K [34] is 2.1 x 10^{-15} m^2/s. Fitting Eq. (5) to the experimental data resulted in a diffusion coefficient of 1.3 x 10^{-12} m^2/s (Table 2), which is three orders of magnitude larger than expected for water droplet diffusion in oil and hence, too large to describe the diffusion of micrometer-sized water droplets in oil. Using the Stokes-Einstein equation, the diffusion coefficient obtained by fitting Eq. (5) corresponded to a hydrodynamic radius r of 34 Å in sunflower oil. Regarding molecular water transport, the diameter of a water molecule is typically in the order of an Å. In case of surfactant facilitated diffusion of water (i.e. water transport by hydrated PGPR molecules or PGPR micelles) [35], the estimated radius strongly depends on the degree of polymerization of the considered PGPR. Using a hydrodynamic radius of a few nanometers for PGPR-facilitated water transport, the diffusion coefficient is in the order of 10^{-11} to 10^{-13} m^2/s. Hence, the hydrodynamic radii as estimated for extra-droplet water diffusion (i.e. molecular water transport or PGPR-facilitated water diffusion) indicate that the obtained diffusion coefficients from Eq. (5) must describe the diffusion of water through the oil layer.

5. Conclusions

A first objective was to evaluate the accuracy of water droplet size analysis of W/O/W emulsions using water diffusion NMR. Low-resolution and high-resolution diffusion NMR were applied to measure the diffusion data of water and the ionic aqueous dissolved marker tetramethylammonium chloride in the water phases of the W/O/W emulsion. Based on the fact that tetramethylammonium chloride has been shown to be an appropriate water soluble marker for NMR studies of emulsions on account of its low permeability through the oil phase in comparison to water [17-19], a previous NMR diffusion study of water and tetramethylammonium chloride in W/O emulsions revealed that the measurement temperature and Δ were crucial aspects towards obtaining more accurate water droplet size analysis using the water diffusion data [8]. It is interesting to find that these aspects were likewise important for W/O/W emulsions, albeit these systems are more complex as obtained upon emulsification of the W/O emulsion into an external water phase. The results depicted a much larger apparent increase in inner water droplet size of the W/O/W emulsion with increasing temperature and Δ in comparison to the use of the marker data.

It was postulated that the different observations between water and the marker were due to a more marked exchange of water through the oil layer inside the oil droplets in comparison to the marker during the diffusion analysis time. Consequently, the use of the latter's diffusion data is thought to approximate the real water droplet radius. Analysis at low temperature and Δ could reduce the droplet size overestimation

using the water diffusion data [6,8,12-14], but we showed that an overestimation was inevitable arising from extra-droplet water diffusion. Whereas a solid crystalline fat phase might slow down the water exchange kinetics in double emulsions [16], we demonstrated that an increased solid fat content of up to 65% was not sufficient to suppress water exchange through the fat layer.

A second objective was to investigate the capability of data analysis procedures to compensate for the effect of extra-droplet water diffusion. In previous studies [6,10], the exchange model was applied that considers exchange between internal and external water. Detailed diffusion analysis revealed that water exchange dominantly occurred between the internal water and the oil phase in our double emulsions during the time frame of the analysis. Therefore, an extension of the exchange model was proposed, but this model could only partly compensate for the effect of exchange in a three phase system. In addition, we showed that the very simple diffusion model, based on Einstein's diffusion law, enabled to regain a diffusion delay independent droplet size from droplet data obtained using a non-exchange model. Hereby, the use of Einstein's diffusion model provided a means to characterize the fat phase permeability of an emulsion, which may be used as an accessory during food product development and quality monitoring.

Acknowledgments

Research funded by a PhD grant (111 508) to L.V. of the Agency for Innovation by Science and Technology (IWT). The authors thank the Fund for Scientific Research – Flanders (FWO Vlaanderen) for their financial support for obtaining the low-resolution 23.4 MHz NMR equipment. We also acknowledge funding from Flanders' Food. Hercules foundation is acknowledged for its financial support in the acquisition of the high-resolution 500 MHz NMR equipment (grant number AUGE-09-006). G.G. would like to thank the Deutsche Forschungsgemeinschaft (DFG) for financial support within the instrumental facility Pro^{2}NMR.

References

[1] E. Dickinson, Food Biophysics 6 (2011) 1-11.

[2] J. P. M. van Duynhoven, G. J. W. Goudappel, G. van Dalen, P. C. van Bruggen, J. C. G. Blonk, A. P. A. M. Eijkelenboom, Magn. Reson. Chem. 40 (2002) S51-S59. DOI: 10.1002/mrc.1115

[3] R. Bernewitz, G. Guthausen, H. P. Schuchmann, Magn. Reson. Chem. 49 (2011) S93-S104. DOI: 10.1002/mrc.2825

[4] R. Bernewitz, U. S. Schmidt, H. P. Schuchmann, G. Guthausen (2014). Colloids Surf. A: Physicochem. Eng. Aspects 458 (2014) 10-18. DOI: 10.1016/j.colsurfa.2014.01.002

[5] P. S. Denkova, S. Tcholakova, N. D. Denkov, K. D. Danov, B. Campbell, C. Shawl, D. Kim, Langmuir 20 (2004) 11402-11413. DOI: 10.1021/la048649v

[6] F. Wolf, L. Hecht, H. P. Schuchmann, E. H. Hardy, G. Guthausen, Eur. J. Lipid Sci. Tech. 111 (2009) 730-742. DOI: 10.1002/ejlt.200800272

[7] X. Guan, K. Hailu, G. Guthausen, F. Wolf, R. Bernewitz, H. P. Schuchmann, Eur. J. Lipid Sci. Tech. 112 (2010) 828–837. DOI: 10.1002/ejlt.201000022

[8] L. Vermeir, P. Sabatino, M. Balcaen, A. Declerck, Dewettinck K., J. C. Martins, P. Van der Meeren, J. Colloid Interface Sci. 463 (2016) 128-136. DOI: 10.106/j.jcis.2015.10.023

[9] J. S. Murday, R. M. Cotts, J. Chem. Phys. 48 (1968) 4938-4945. DOI: 10.1063/1.1668160

[10] J. P. Hindmarsh, J. Su, J. Flanagan, H. Singh, Langmuir 21 (2005) 9076-9084. DOI: 10.1021/la051626b

[11] L. Vermeir, M. Balcaen, P. Sabatino, K. Dewettinck, P. Van der Meeren, Colloids Surf. A: Physicochem. Eng. Aspects 456 (2014) 129–138. DOI: 10.1016/j.colsurfa.2014.05.022

[12] B. Balinov, P. Linse, O. Söderman, J. Colloid Interface Sci. 182 (1996) 539-548. DOI: 10.1006/jcis.1996.0498

[13] I. Fourel, J. P. Guillement, D. Le Botlan, J. Colloid Interface Sci. 164 (1994) 48-53. DOI: 10.1006/jcis.1994.1142

[14] J. C. Van den Enden, D. Waddington, H. van Aalst, C. G. Van Kralingen, K. J. Packer, J. Colloid Interface Sci. 140 (1990) 105-113. DOI: 10.1016/0021-9797(90)90327-K

[15] J. Pfeuffer, U. Flögel, W. Dreher, D. Leibfritz, NMR Biomed. 11 (1998) 19-31. DOI:

10.1002/(SICI)1099-1492(199802)11:1<19::AID-NBM499>3.0.CO;2-O

[16] R. Mezzenga, Food Hydrocoll. 21 (2007) 674–682. DOI: 10.1016/j.foodhyd.2006.08.019

[17] S. Lasič, I. Åslund, D. Topgaard, J. Magn. Reson. 199 (2009) 166–172. DOI: 10.1016/j.jmr.2009.04.014

[18] N. N. Yadav, W. S. Price, J. Colloid Interface Sci. 338 (2009) 163-168. DOI: 10.1016/j.jcis.2009.06.014

[19] C. Malmborg, D. Topgaard, O. Söderman, J. Colloid Interface Sci. 263 (2003) 270–276. DOI: 10.1016/S0021-9797(03)00259-5

[20] J. Su, J. Flanagan, Y. Hemar, H. Singh, Food Hydrocoll. 20 (2006) 261-268. DOI: 10.1016/j.foodhyd.2004.03.010

[21] J. P. M. van Duynhoven, B. Maillet, J. Schell, M. Tronquet, G. J. W. Goudappel, E. Trezza, A. Bulbarello, D. van Dusschoten, Eur. J. Lipid Sci. Tech. 109 (2007) 1095–1103. DOI: 10.1002/ejlt.200700019

[22] H. J. Motulsky, L. A. Ransnas, FASEB J. 1 (1987) 365–374.

[23] M. L. Johns, Curr. Opin. Colloid Interface Sci. 14 (2009) 178–183.

[24] M. A. Voda, J. P. M. van Duynhoven, Trends Food Sci. Tech. 20 (2009) 533-543. DOI: 10.1016/j.tifs.2009.07.001

[25] K. J. Packer, C. J. Rees, J. Colloid Interface Sci. 40 (1972) 2, 216-218.

[26] S. M. Schoberth, N.-K. Bär, R. Krämer, J. Kärger, Anal. Biochem. 279 (2000) 100-105. DOI: 10.1006/abio.1999.4450

[27] S. So, T. P. Lodge, J. Phys. Chem. C 118 (2014) 21140-21147. DOI: 10.1021/jp50518h

[28] J. Cheng, J.-F. Chen, M. Zhao, Q. Luo, L. Wen, K. D. Papadopoulos, J. Colloid Interface Sci. 305 (2007) 175-182. DOI: 10.1016/j.jcis.2006.09.055

[29] M. H. Hilder, JAOCS 45 (1968) 703-707. DOI: 10.1007/BF02541262

[30] M. H. Hilder, M. van den Tempel, J. Appl. Chem. Biotechn. 21 (1971) 176-179.

[31] M. L. Johns, K. G. Hollingsworth, Prog. Nucl. Mag. Res. Sp. 50 (2007) 51–70. DOI: 10.1016/j.pnmrs.2006.11.001

[32] S. Kiokias, A. A. Reszka, A. Bot, Int. Dairy J. 14 (2004) 287-295. DOI: 10.1016/j.idairyj.2003.09.007

[33] A. Einstein, Annalen der Physik 17 (1905) 549-560.

[34] L. M. Diamante, T. Lan, J. Food Processing (2014) 1-6. DOI: 10.1155/2014/234583

[35] L. Wen, K. D. Papadopoulos, Colloids Surf. A: Physicochem. Eng. Aspects 174 (2000) 159-167. DOI: 10.106/S0927-7757(00)00508-2

Figure captions

Fig. 1. Schematically drawn systems. (a) W/O/W emulsion with negligible exchange between the inner water droplets, as well as between the inner water droplets and the external water phase. (b) W/O/W emulsion with negligible exchange between the inner (p_1) and outer water phase (p_3) and mean residence time τ_1 and τ_2 in p_1 (W_1) and p_2 (oil), respectively.

Fig. 2. (a) Simulated normalized echo decay of a W/O/W emulsion (and inset at small q^2) using Eq. (3), $D_2 = 1.1 \times 10^{-9}$ m^2/s, $p_2 = 0.75$, $\tau_1 = 0.1$ s (– · –) for $\Delta = 140$ ms (grey) and $\Delta = 220$ ms (black). Using Eq. (4), with EV = 25%, $D_2 = 0.4 \times 10^{-9}$ m^2/s, $p_2 = 0.01$ and $D_3 = 1.1 \times 10^{-9}$ m^2/s, the following echo decays were simulated for $\tau_1 = 0.1$ s (—) and $\Delta = 60$ ms (light grey), $\Delta = 140$ ms (grey) and $\Delta = 220$ ms (black); $\tau_1 = 30$ s and $\Delta = 60$ ms (– –); $\tau_1 = 30$ s and $\Delta = 220$ ms (···). For both equations, the values of δ, R_{43}, σ, and I_0 were set at 2.5 ms, 1.50 µm, 0.25 µm and 1, respectively. (b) Experimentally obtained normalized echo decay of the sodium caseinate stabilized W/O_s/W emulsion as measured at 35 °C using low-resolution NMR. Full lines represent the fitting of Eq. (4) to the experimentally obtained diffusion data at a diffusion delay Δ (60-140-220 ms).

Fig. 3. Normalized echo intensity of water (triangles) and TMACl (squares) in the W/O/W emulsion as measured at 5 °C using $\Delta = 600$ ms by high-resolution NMR. The lines represent the fitting of Eq. (1) to the diffusion data.

Fig. 4. Effect of diffusion delay value Δ (250-450-600 ms) on the normalized echo intensity of (a) water and (b) TMACl in the W/O/W emulsion as measured at 25 °C with high-resolution NMR. The lines represent the fitting of Eq. (1) to the diffusion data.

Fig. 5. Effect of measurement temperature and diffusion delay on the estimated R_{43}-value of the W/O/W emulsion as based on water (circles) and TMACl (diamonds) diffusion data using HR-NMR and $\Delta = 600$ ms (black filled markers), $\Delta = 450$ ms (grey filled markers) and $\Delta = 250$ ms (empty markers). Also the radius obtained from the LR-diffusion data at 600 ms (∗) is included. Lines represent a guide to the eye.

Fig. 6. Echo intensity of water in the W/O_s/W emulsion as measured at 5 °C (a) and 35 °C (b). Full lines represent the fitting of Eq. (1), whereas the dashed-dotted lines refer to the fitting using Eq. (4) to the experimentally obtained diffusion data (markers) at a diffusion delay Δ of 60 ms (diamonds), 80 ms (crosses), 100 ms (triangles), 140 ms (circles) and 220 ms (squares).

Fig. 7. Effect of measurement temperature and diffusion delay Δ on the estimated R_{43}-value upon fit of Eq. (1) (solid markers) or Eq. (4) (empty circles) to the water diffusion data of the (a) $W/O_s/W$ emulsion and (b) $W/O_h/W$ emulsion using LR-NMR. Einstein's diffusion law fit of Eq. (5) (crosses) to the fitted results from Eq. (1) are also included. Dotted lines represent a guide to the eye.

Fig. 8.

Fit of Einstein's diffusion law using Eq. (5) (lines) to the apparent water droplet radius R_{43} of the $W/O_h/W$ emulsion as obtained from Eq. (1) (markers) using different Δ values and temperatures.

Table 1

Best fitted values for the residence time of water molecules within the internal water droplets (τ_1) for the W/O/W emulsion using Eq. (4).

	τ_1 (s)	
T (°C)	$W/O_s/W$	$W/O_h/W$
5	1.00 ± 0.27	1.57 ± 2.61
15	0.79 ± 0.16	0.44 ± 2.80
25	0.33 ± 0.14	0.56 ± 0.23
35	0.09 ± 0.09	0.30 ± 0.11

Table 2

Output of Einstein's diffusion law fit (Eq. (5)) to the R_{43}-values of the W/O/W emulsion as obtained from Eq. (1). Questionable fitting of the $W/O_s/W$ data at 25 °C are placed between brackets.

	$R_{43,0}$ (μm)		D (10^{-11} m^2/s)	
T (°C)	$W/O_s/W$	$W/O_h/W$	$W/O_s/W$	$W/O_h/W$
5	0.92 ± 0.13	2.03 ± 0.13	0.11 ± 0.11	0.01 ± 0.02
15	1.10 ± 0.08	1.96 ± 0.17	0.14 ± 0.05	0.05 ± 0.08
25	(2.76 ± 0.24)	2.06 ± 0.14	(0.06 ± 0.11)	0.13 ± 0.10
35	1.35 ± 0.10	1.91 ± 0.22	1.72 ± 0.29	0.65 ± 0.41

Fig.1a

Fig. 1a

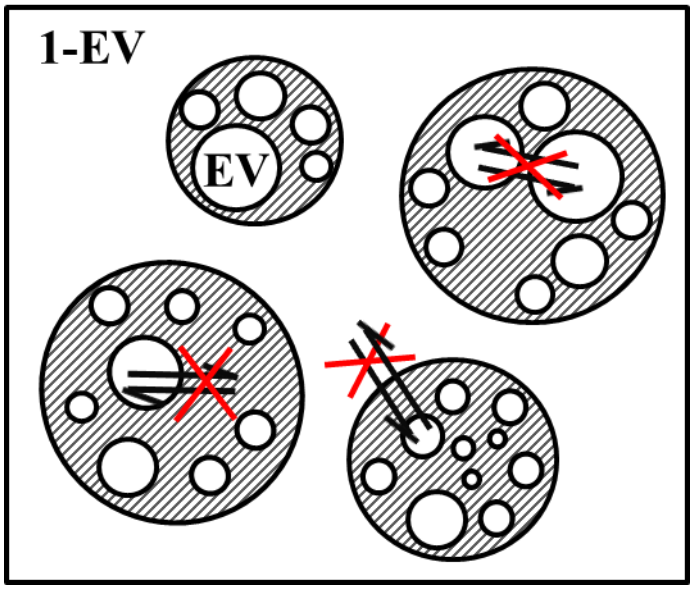

Fig.1a

Click here to download high resolution image

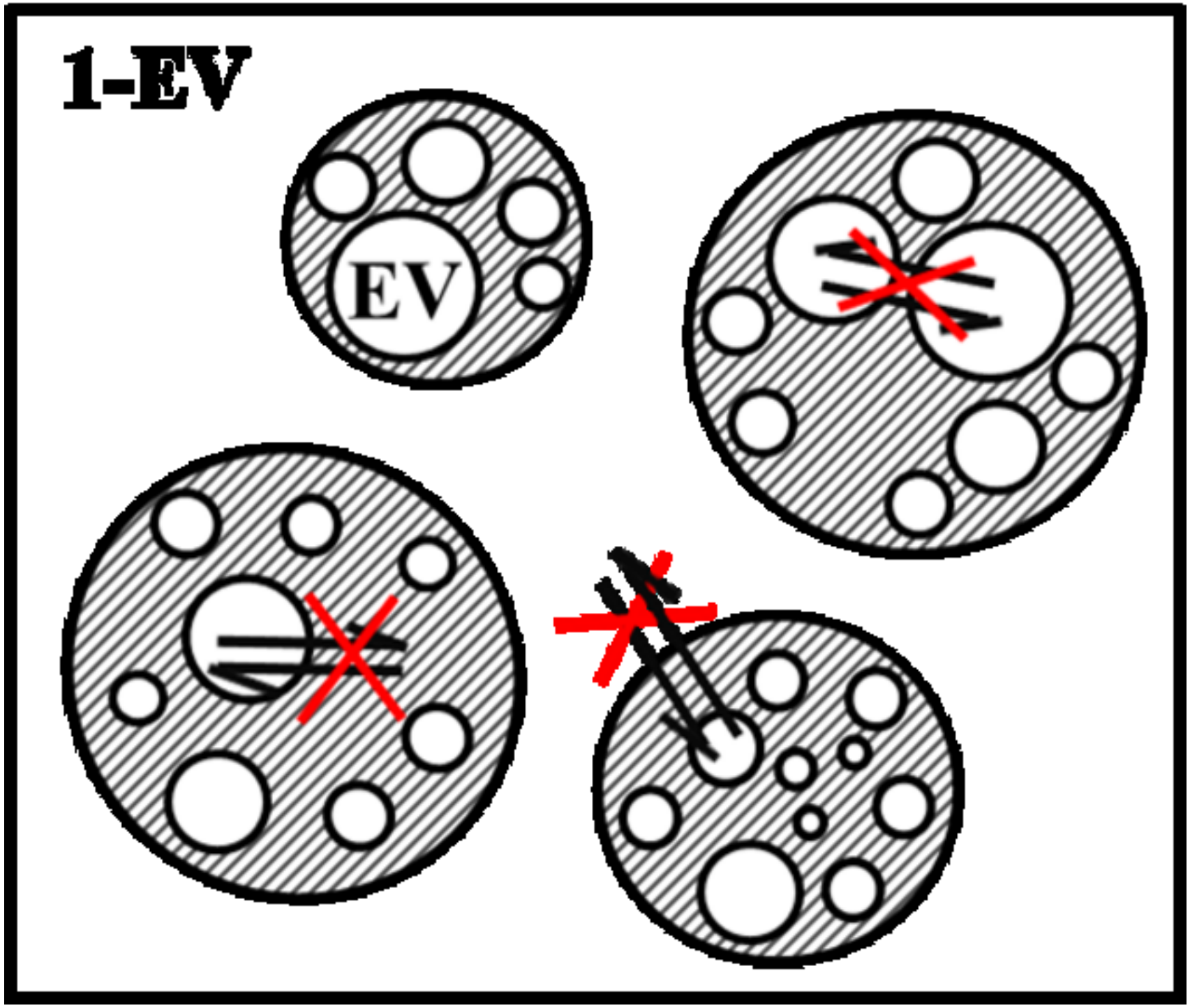

Fig.1b

Fig. 1b

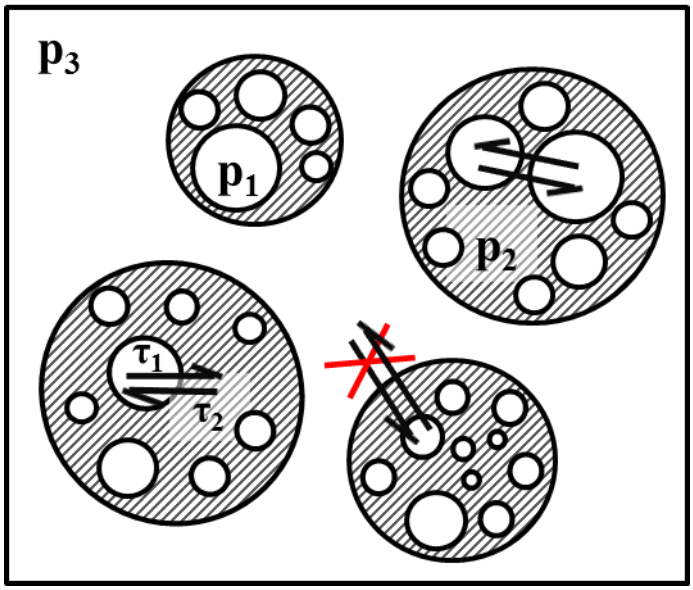

Fig.1b

Click here to download high resolution image

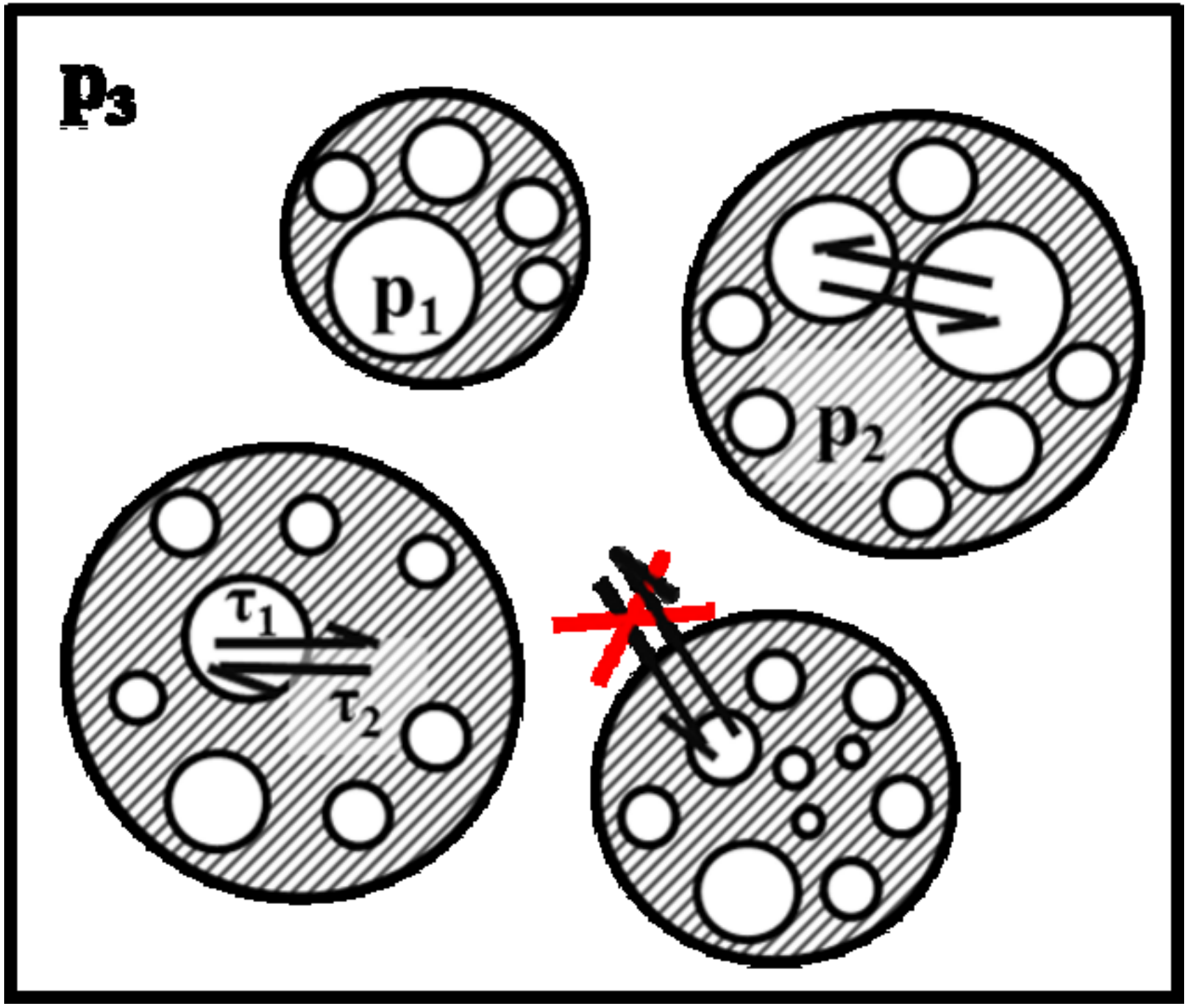

Fig.2a

Fig. 2a

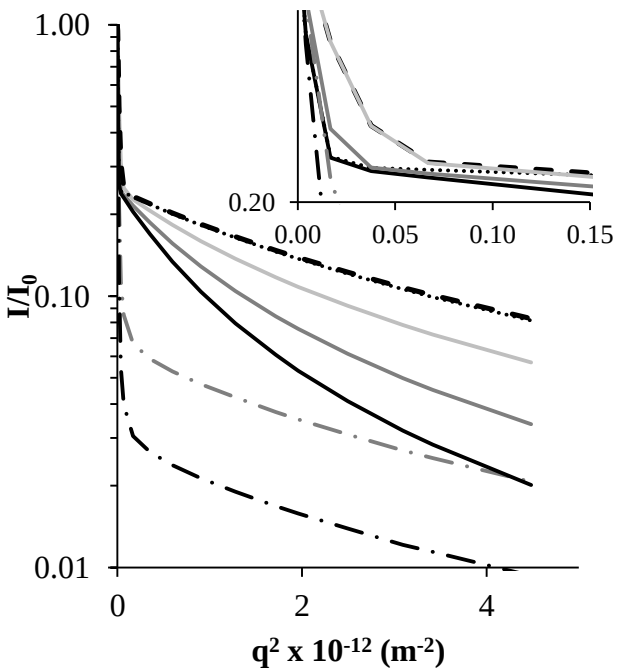

Fig.2a

Click here to download high resolution image

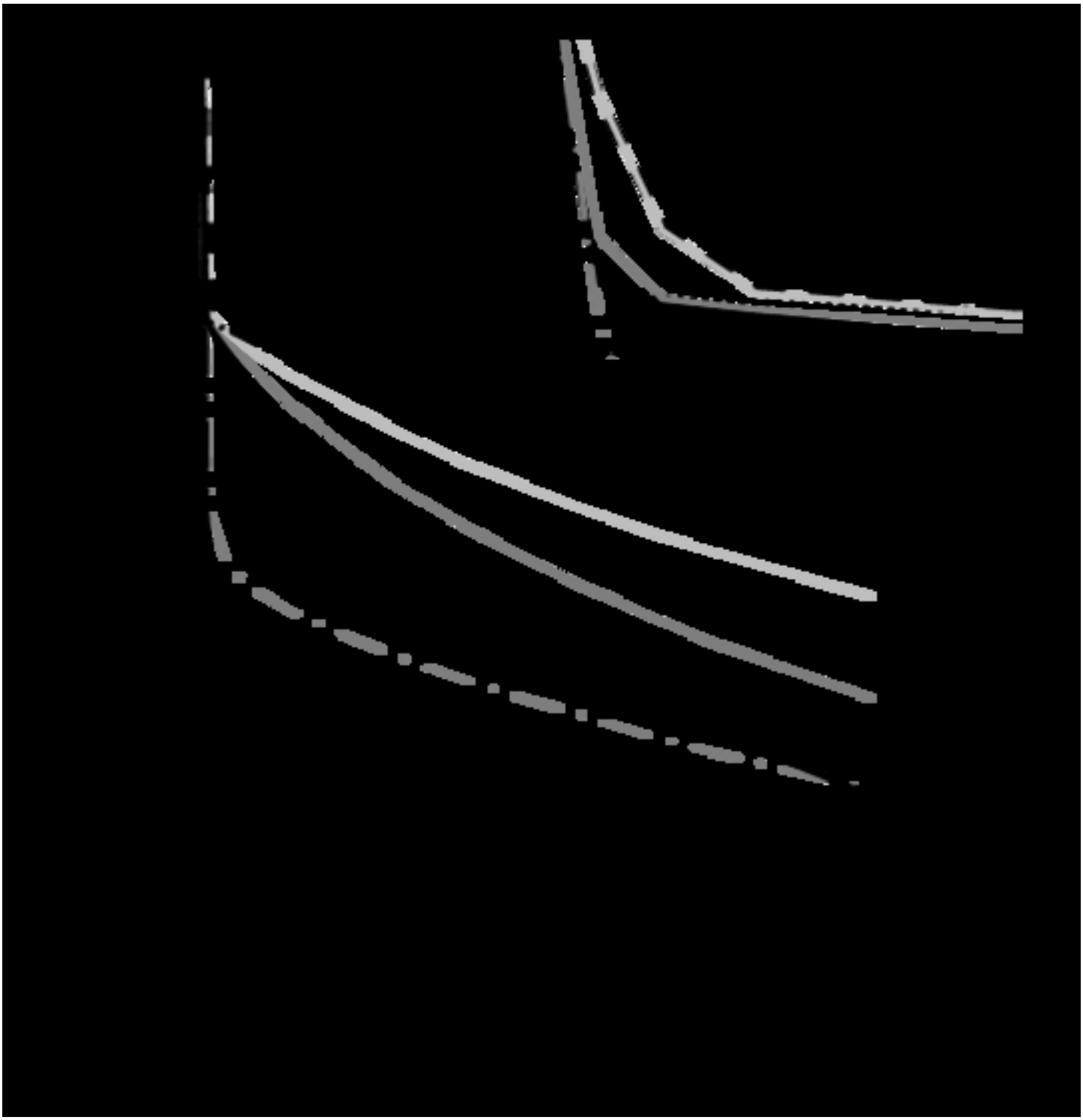

Fig.2b

Fig. 2b

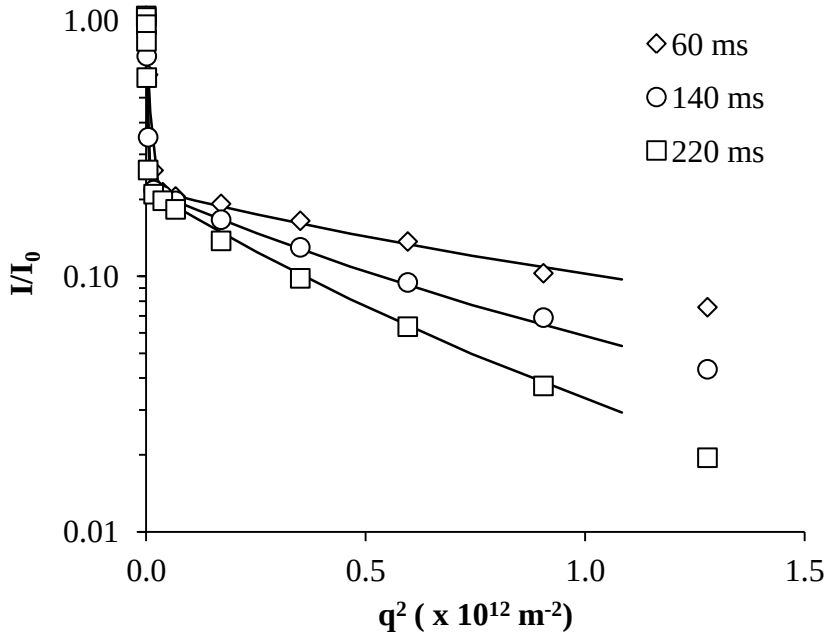

Fig.2b

Click here to download high resolution image

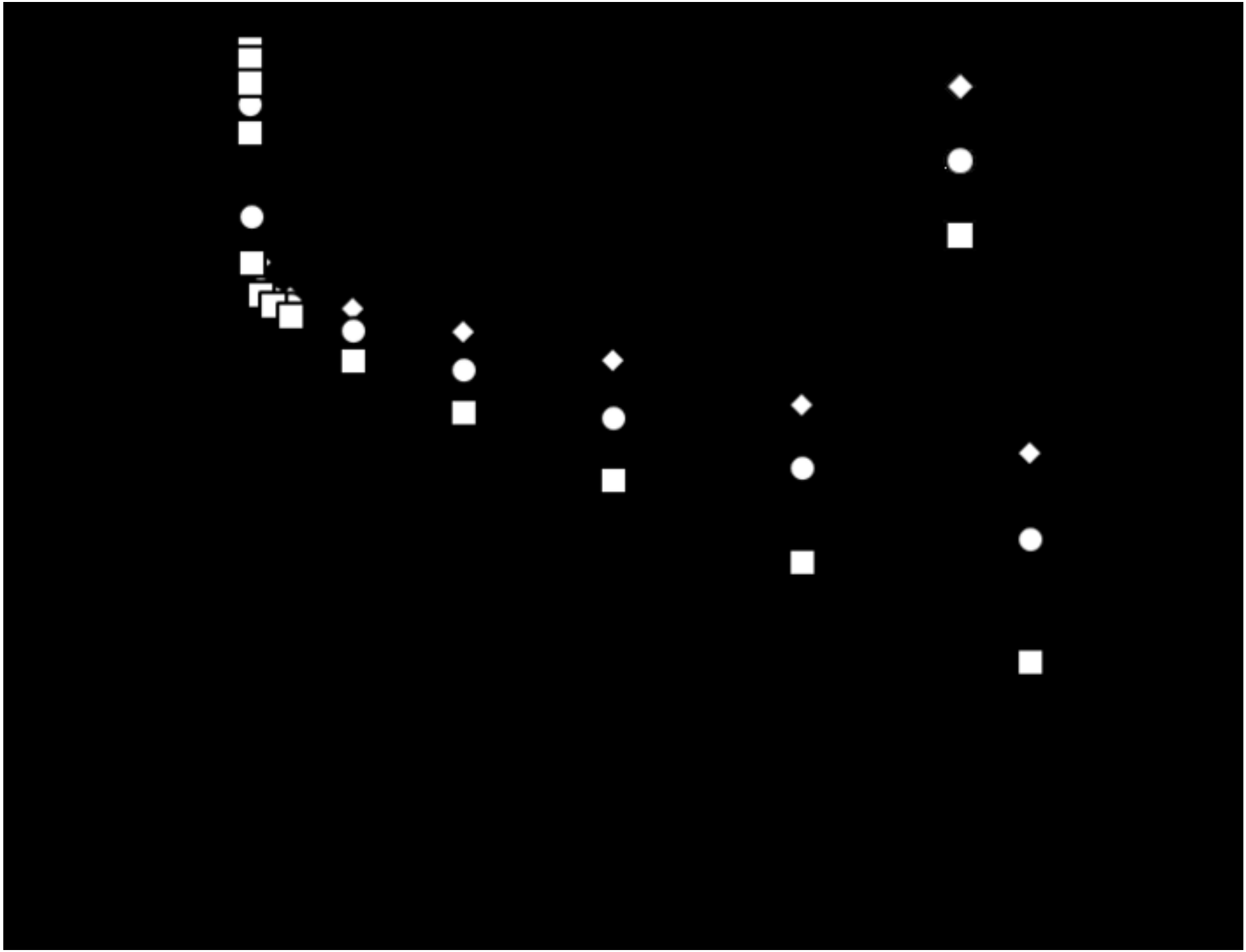

Fig.3

Fig. 3

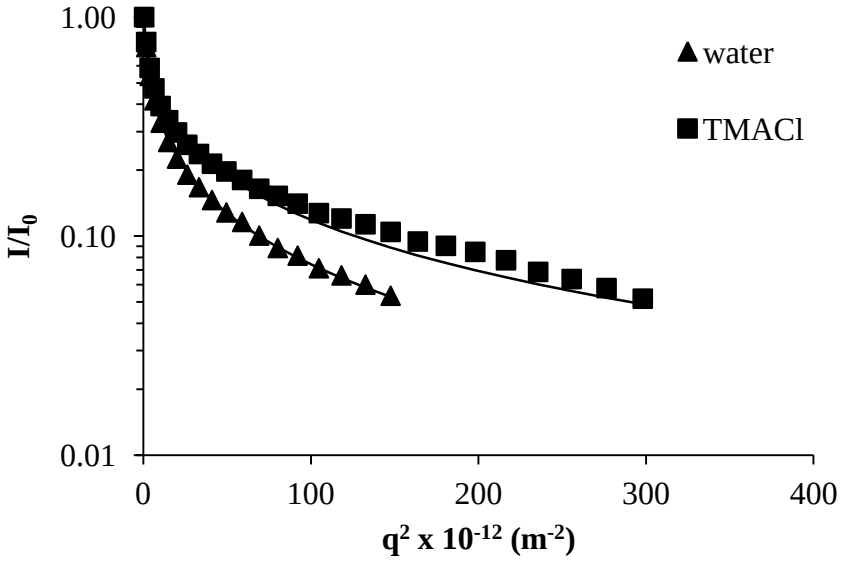

Fig.3

Click here to download high resolution image

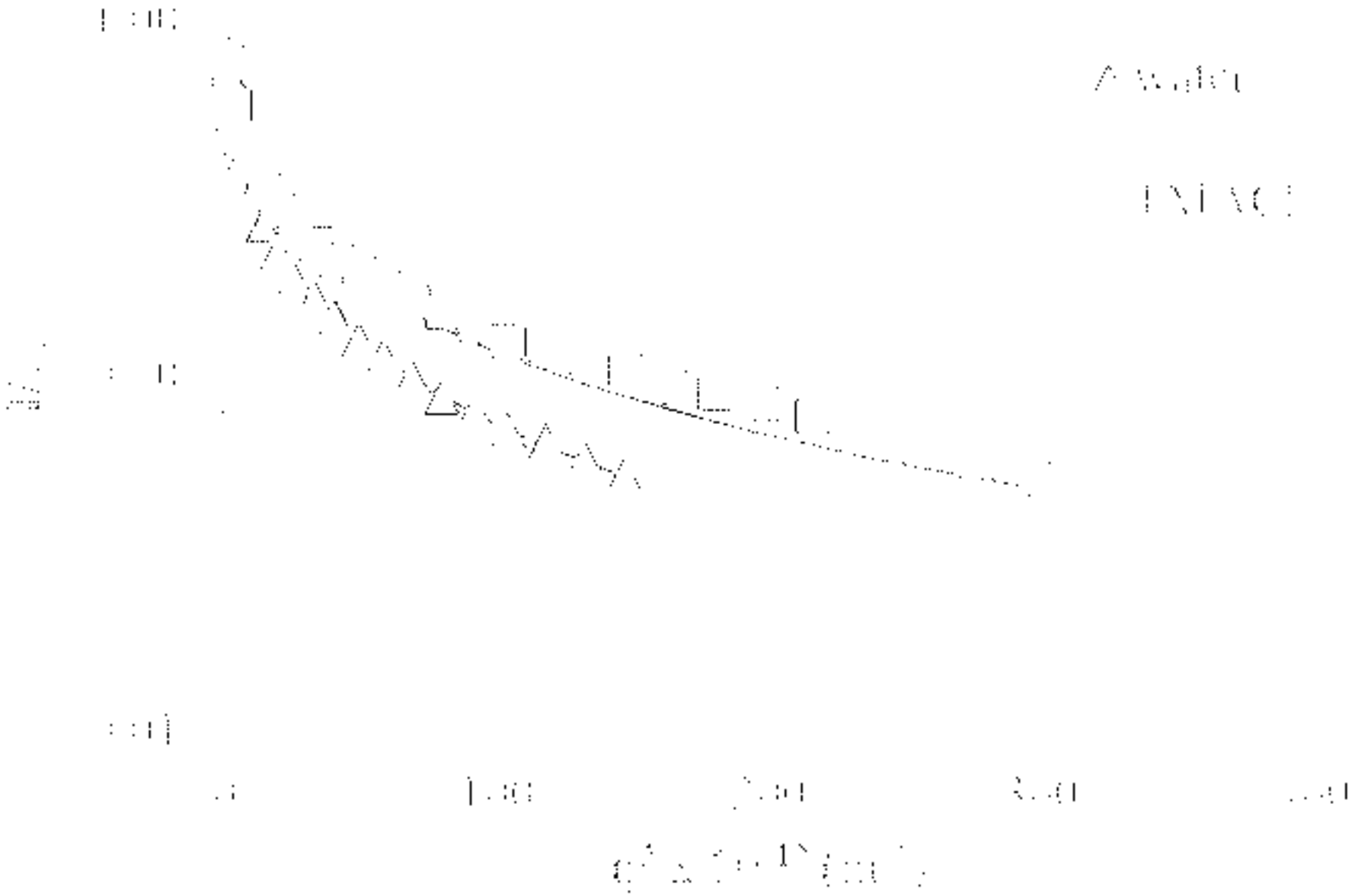

Fig.4a

Fig. 4a

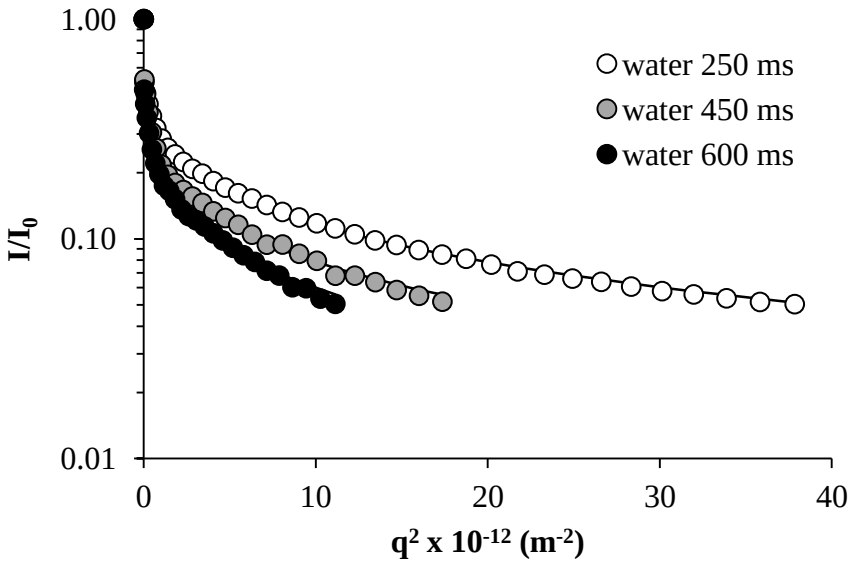
1.00
0.10
0.01
I/I0
0
10
20
30
40
q2 x 10-12 (m-2)
water 250 ms
water 450 ms
water 600 ms

Fig.4a

Click here to download high resolution image

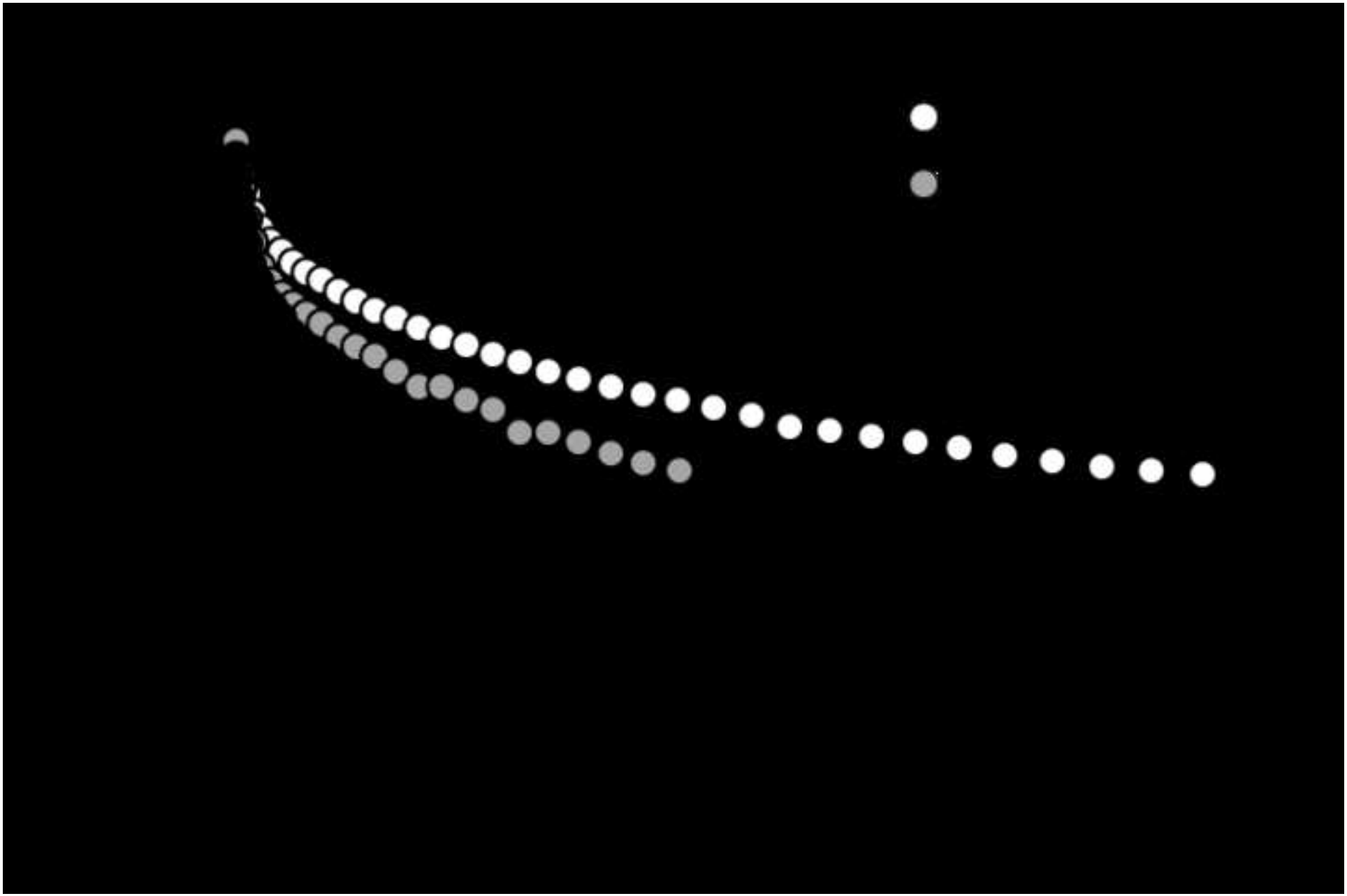

Fig.4b

Fig. 4b

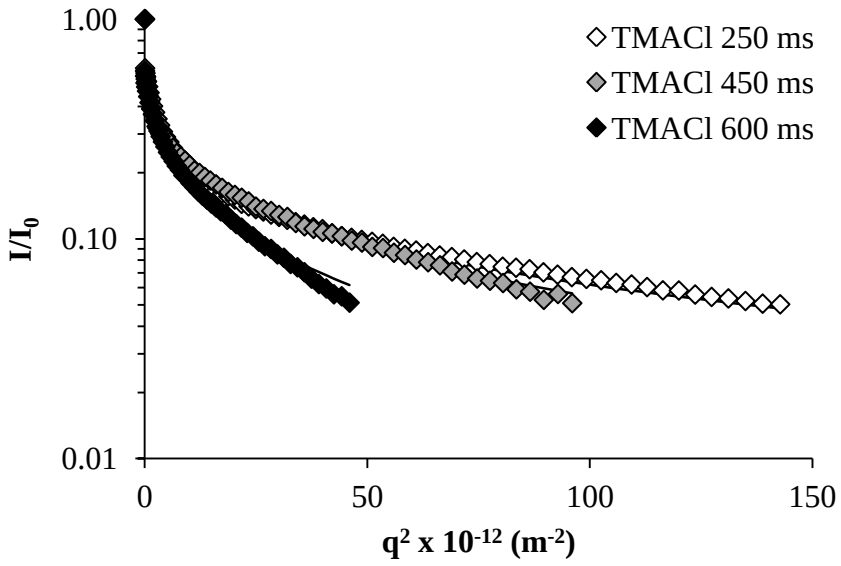
1.00
0.10
0.01
I/I0
0
50
100
150
q2 x 10-12 (m-2)
TMACl 250 ms
TMACl 450 ms
TMACl 600 ms

Fig.4b

Click here to download high resolution image

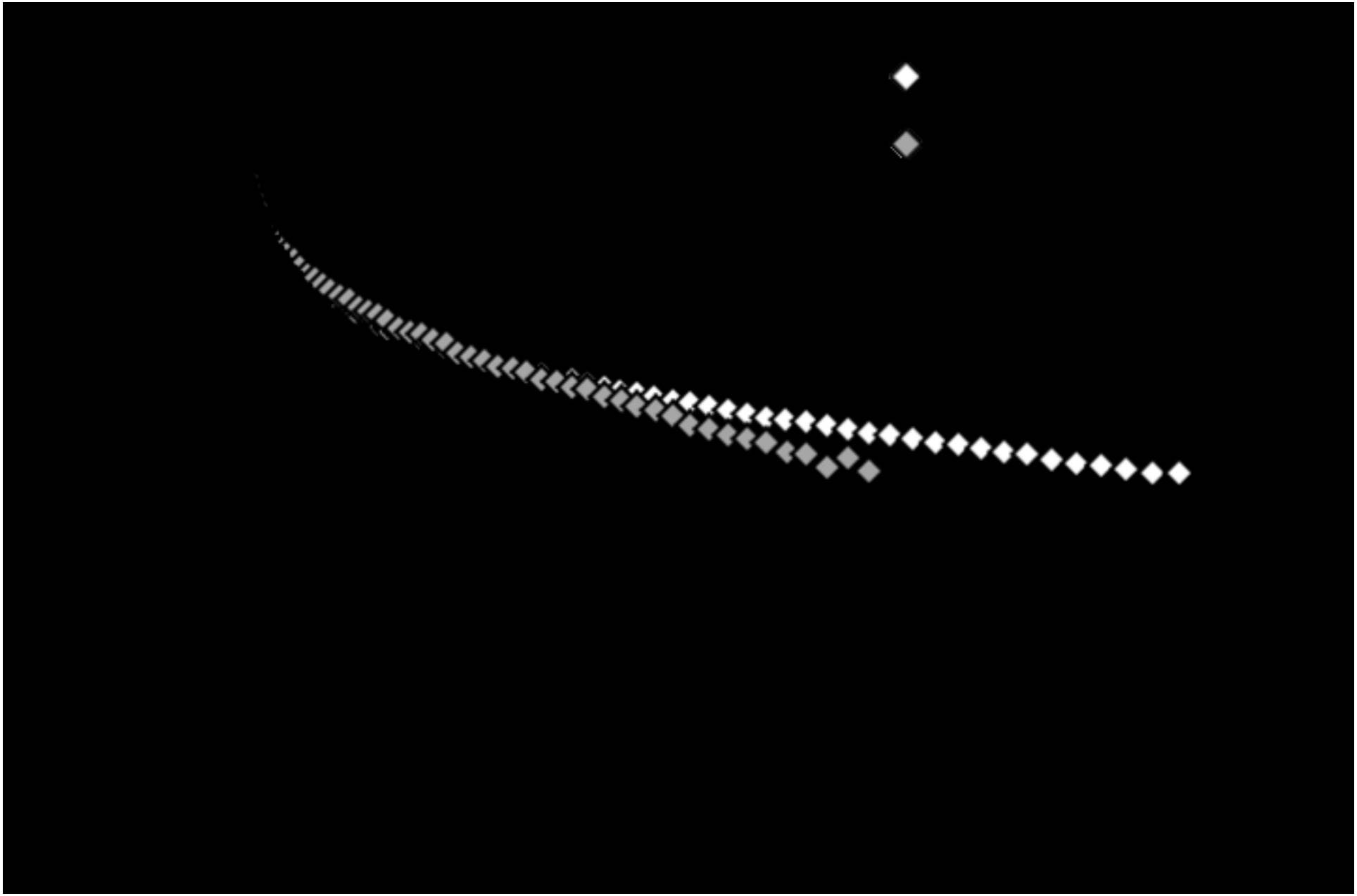

Fig.5

Fig. 5

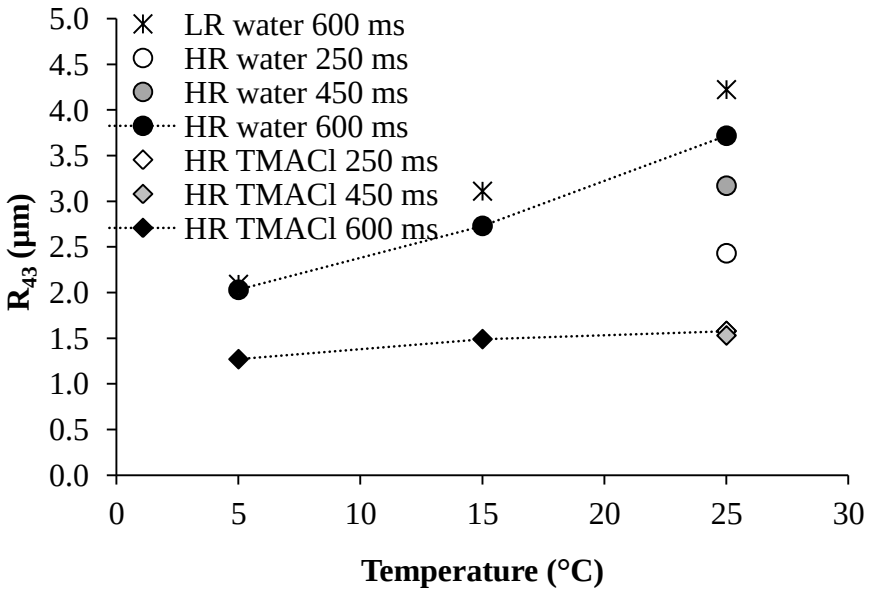
LR water 600 ms
HR water 250 ms
HR water 450 ms
HR water 600 ms
HR TMACl 250 ms
HR TMACl 450 ms
HR TMACl 600 ms
R_{43} (µm)
Temperature (°C)
0.0
0.5
1.0
1.5
2.0
2.5
3.0
3.5
4.0
4.5
5.0
0
5
10
15
20
25
30

Fig.5

Click here to download high resolution image

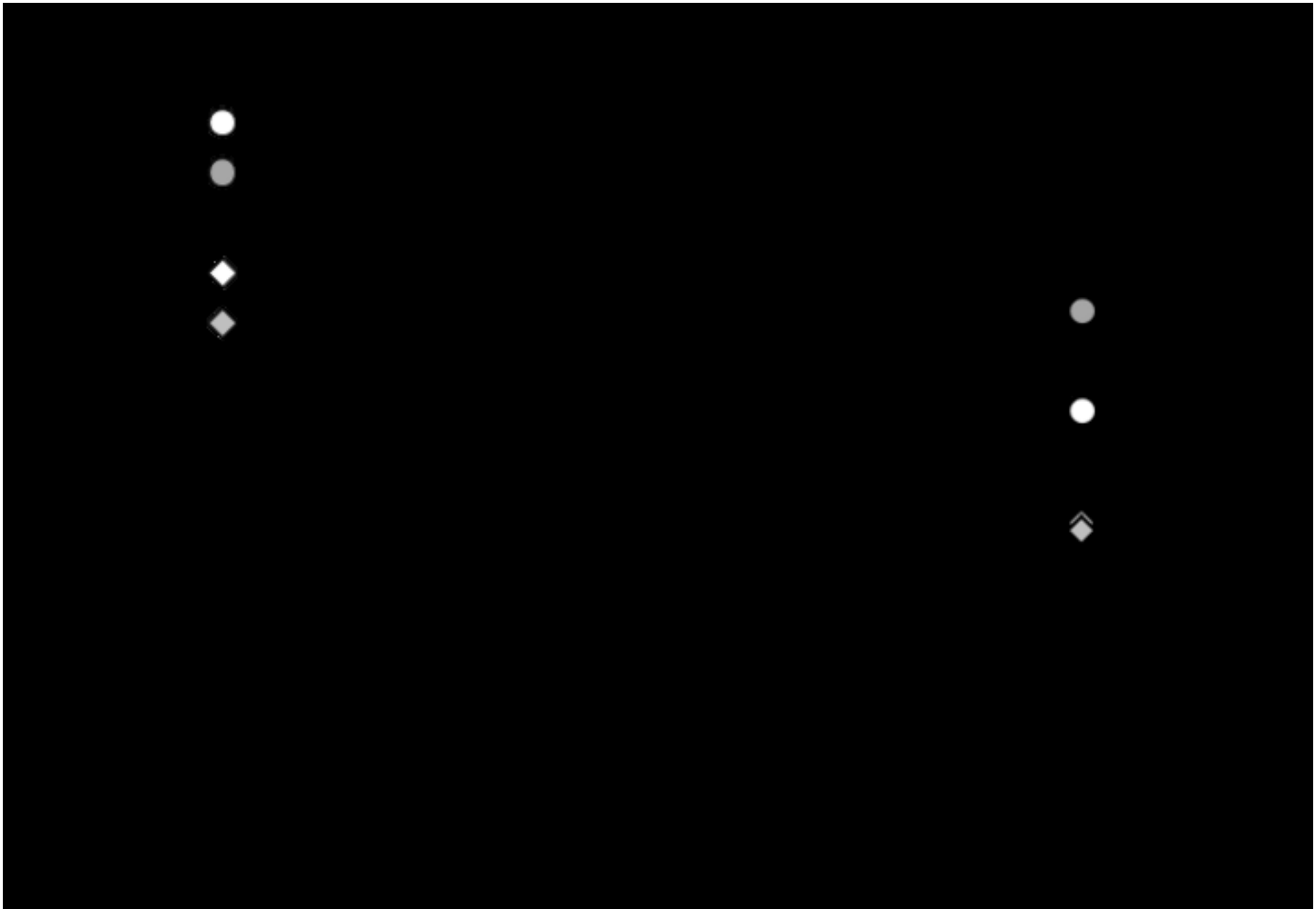

Fig.6a

Fig. 6a

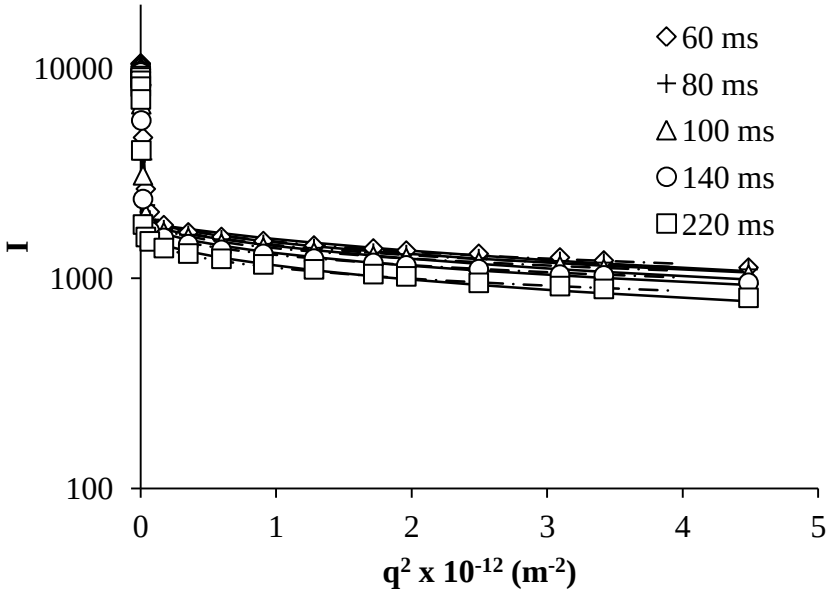
60 ms
80 ms
100 ms
140 ms
220 ms
10000
1000
100
I
0
1
2
3
4
5
q2 x 10-12 (m-2)

Fig.6a

Click here to download high resolution image

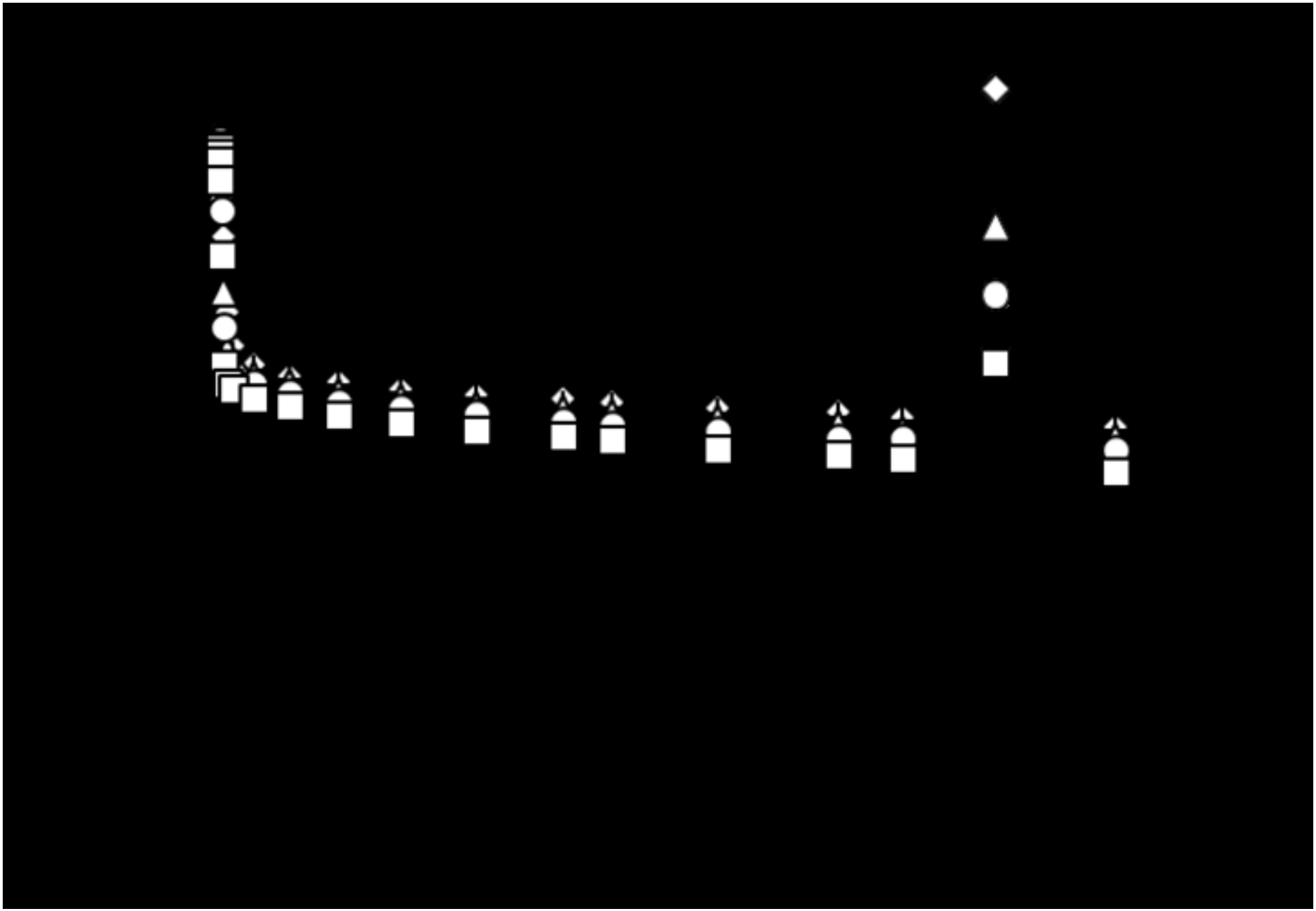

Fig.6b

Fig. 6b

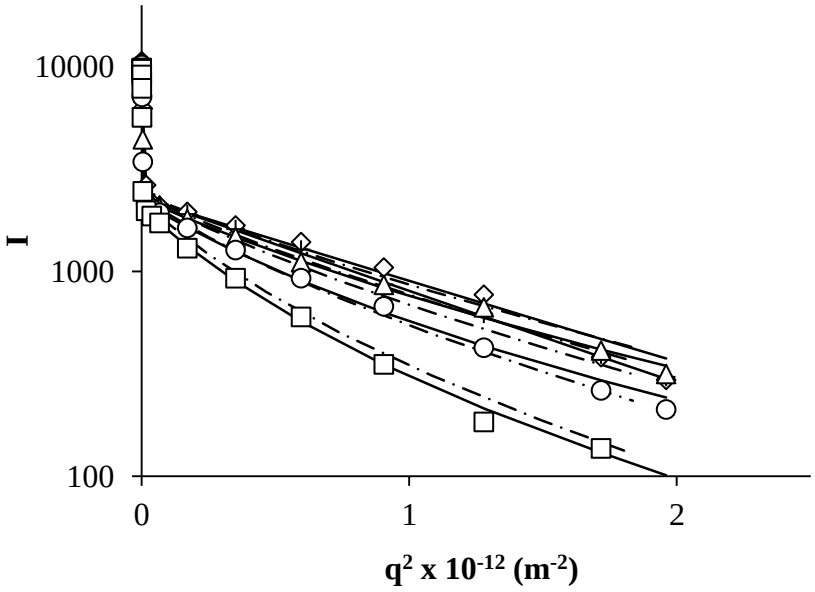

Fig.6b

Click here to download high resolution image

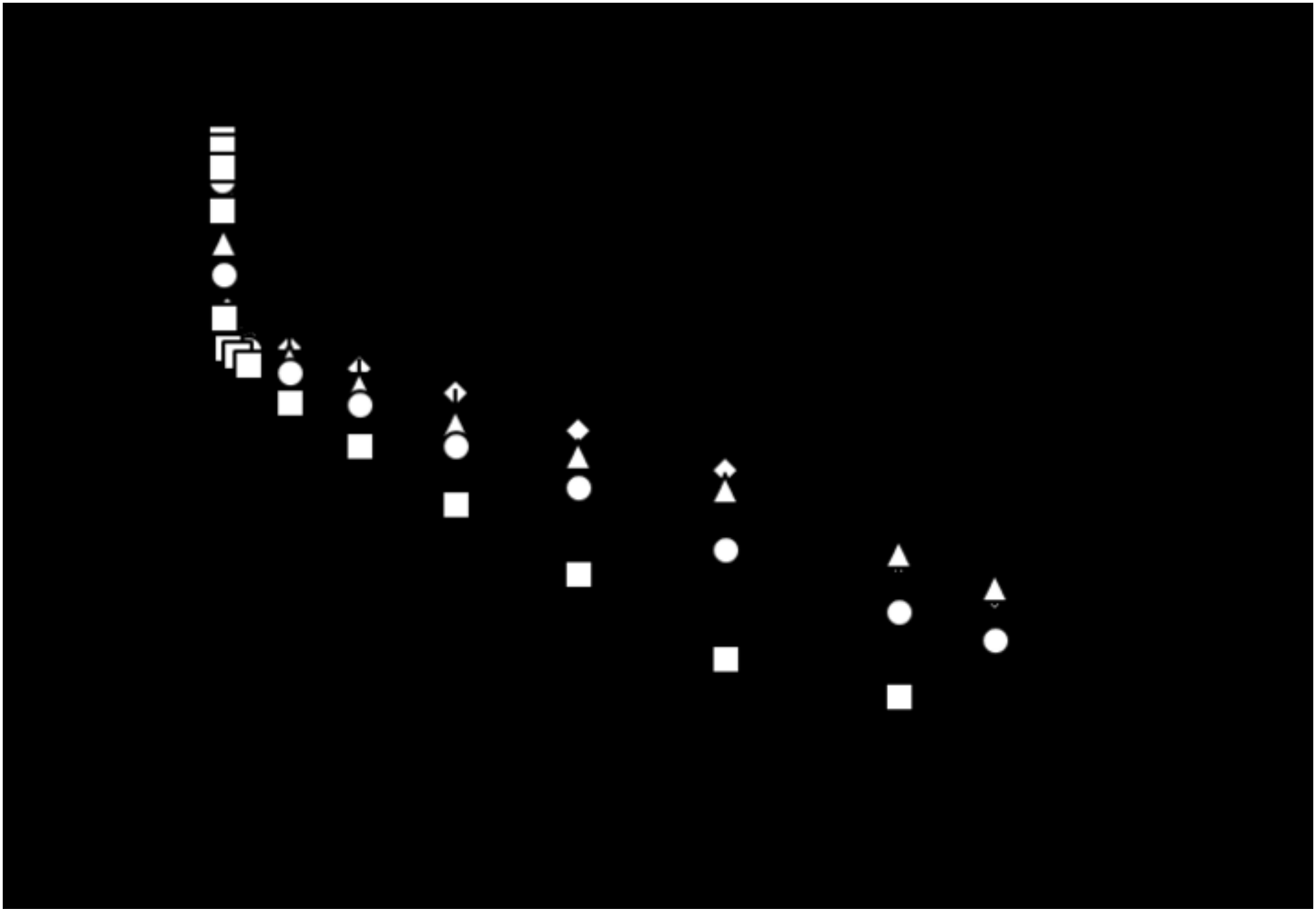

Fig.7a

Fig. 7a

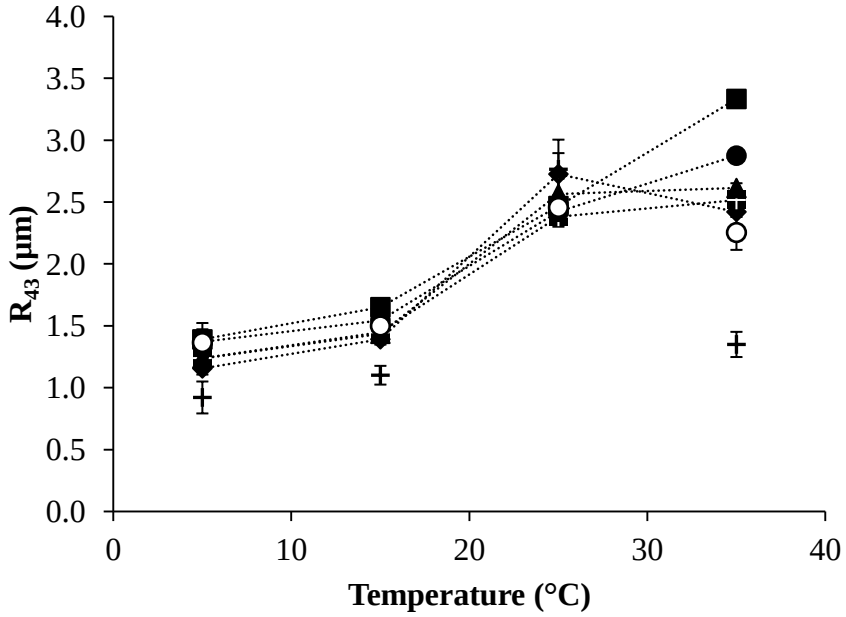

Fig.7a

Click here to download high resolution image

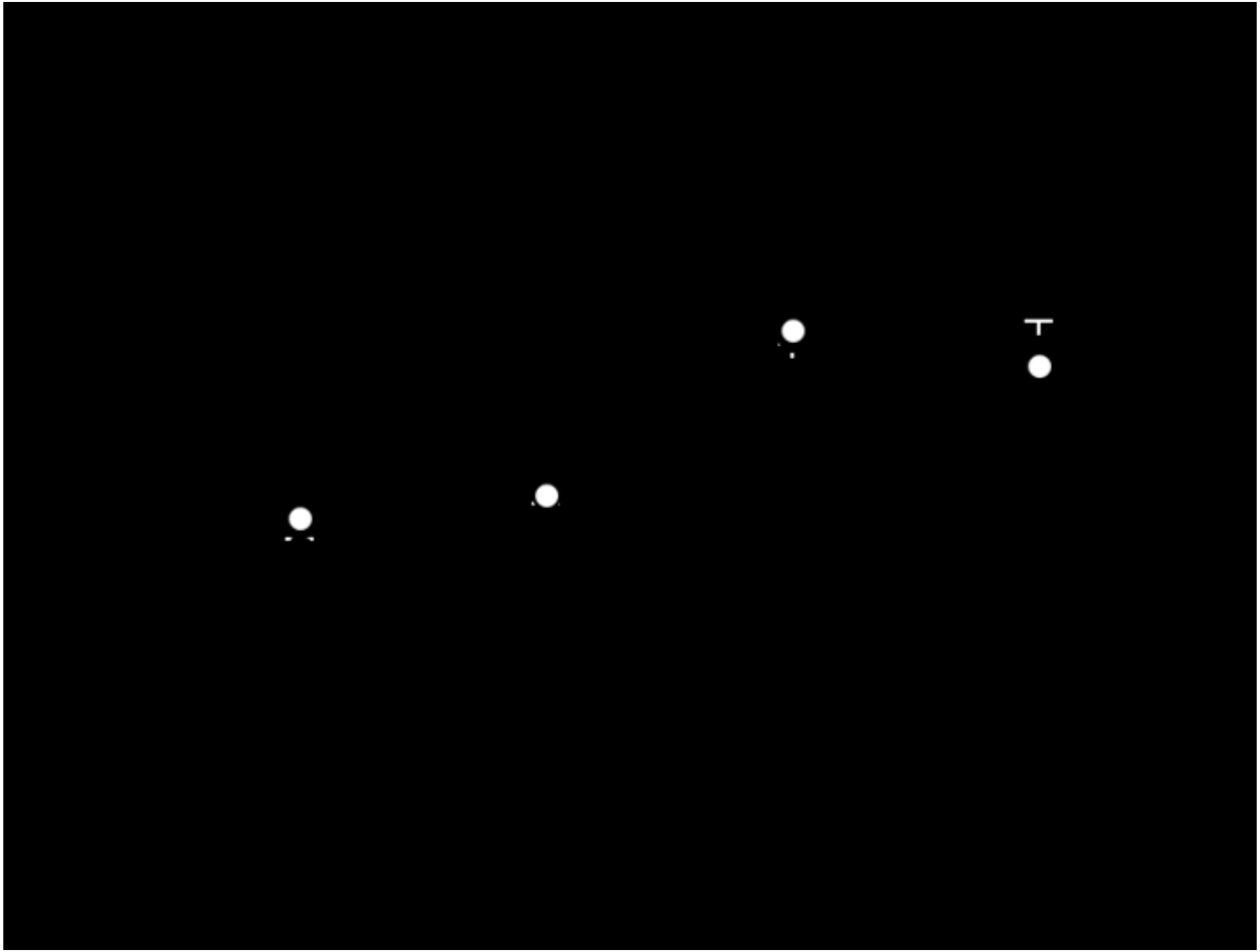

Fig. 7b

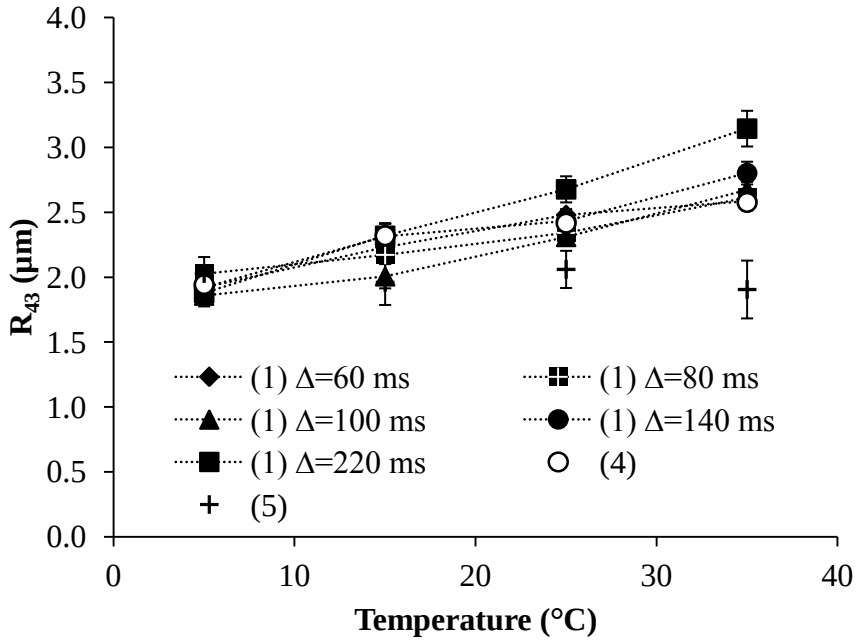
4.0
3.5
3.0
2.5
2.0
1.5
1.0
0.5
0.0
R_{43} (µm)
0
10
20
30
40
Temperature (°C)
(1) Δ=60 ms
(1) Δ=80 ms
(1) Δ=100 ms
(1) Δ=140 ms
(1) Δ=220 ms
(4)
(5)

Fig.7b

Click here to download high resolution image

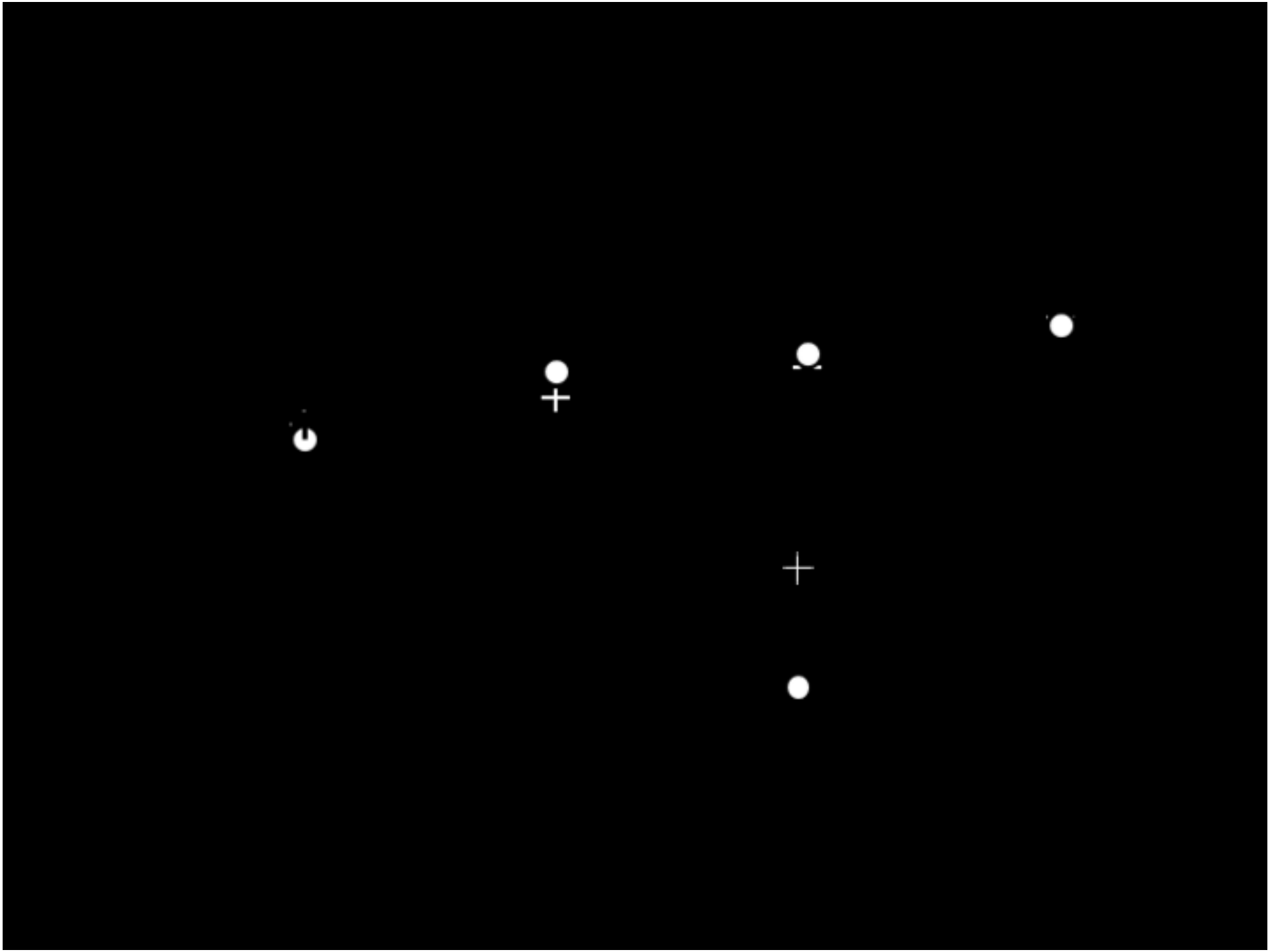

Fig. 8

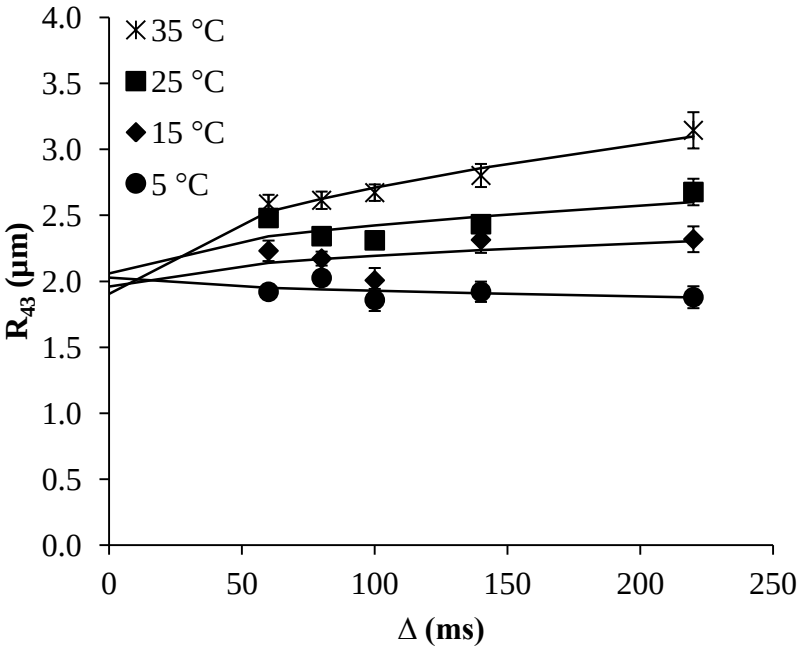
35 °C
25 °C
15 °C
5 °C
4.0
3.5
3.0
2.5
2.0
1.5
1.0
0.5
0.0
R43 (µm)
0
50
100
150
200
250
Δ (ms)

Fig.8

Click here to download high resolution image

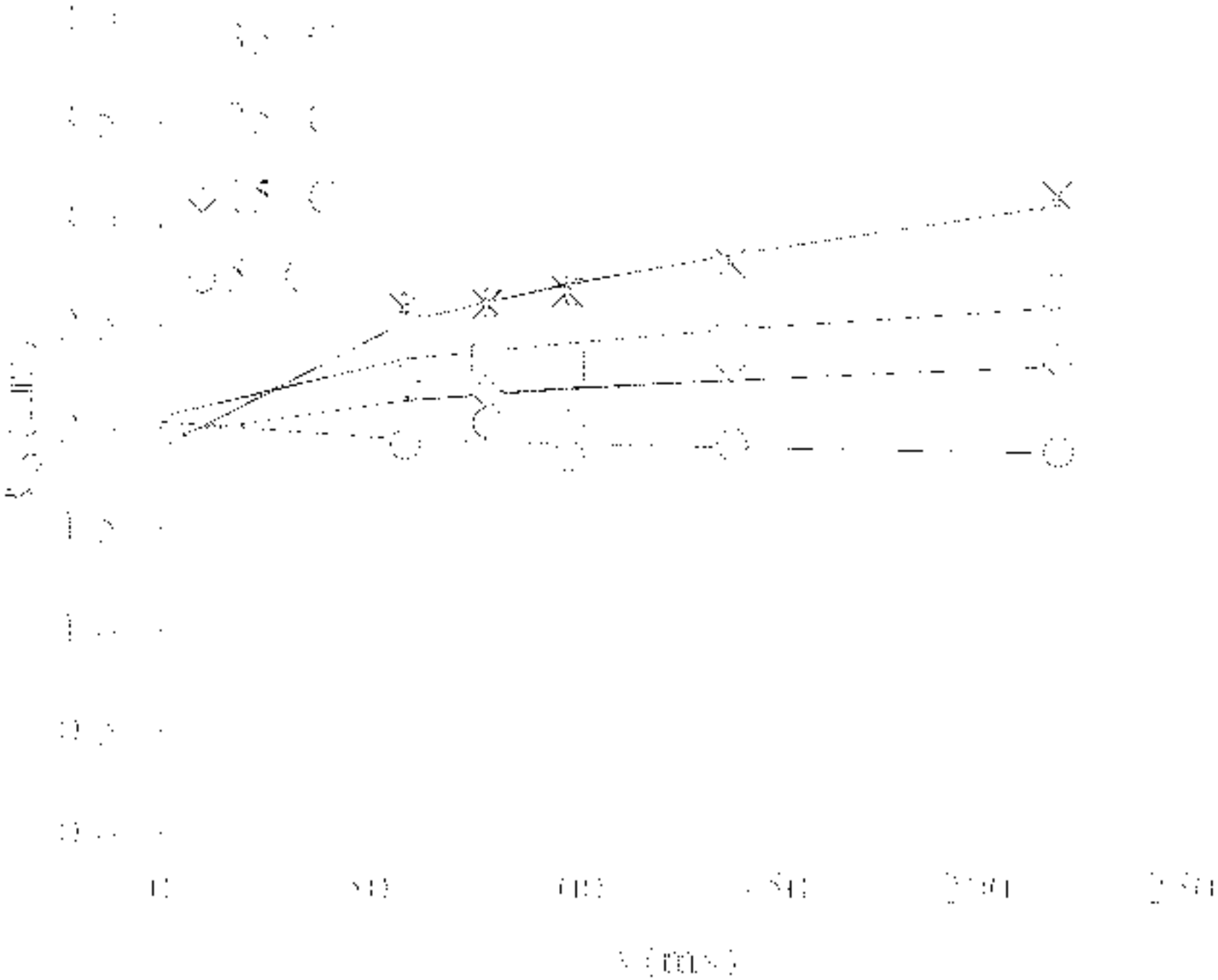

Table 1

Best fitted values for the residence time of water molecules within the internal water droplets (τ_1) for the W/O/W emulsion using Eq. (4).

	τ_1 (s)	
T (°C)	$W/O_s/W$	$W/O_h/W$
5	1.00 ± 0.27	1.57 ± 2.61
15	0.79 ± 0.16	0.44 ± 2.80
25	0.33 ± 0.14	0.56 ± 0.23
35	0.09 ± 0.09	0.30 ± 0.11

Table 2

Output of Einstein's diffusion law fit (Eq. (5)) to the R_{43}-values of the W/O/W emulsion as obtained from Eq. (1). Questionable fitting of the $W/O_s/W$ data at 25 °C are placed between brackets.

	$R_{43,0}$ (μm)		D (10^{-11} m^2/s)	
T (°C)	$W/O_s/W$	$W/O_h/W$	$W/O_s/W$	$W/O_h/W$
5	0.92 ± 0.13	2.03 ± 0.13	0.11 ± 0.11	0.01 ± 0.02
15	1.10 ± 0.08	1.96 ± 0.17	0.14 ± 0.05	0.05 ± 0.08
25	(2.76 ± 0.24)	2.06 ± 0.14	(0.06 ± 0.11)	0.13 ± 0.10
35	1.35 ± 0.10	1.91 ± 0.22	1.72 ± 0.29	0.65 ± 0.41